Coupled Systems Mechanics, *Vol. 11, No. 2 (2022) 167-198*
https://doi.org/10.12989/csm.2022.11.2.167

Instability of (Heterogeneous) Euler beam: Deterministic vs. stochastic reduced model approach

Adnan Ibrahimbegovic*[1,3], Rosa Adela Mejia-Nava[1],
Emina Hajdo[2] and Nikolaos Limnios[4]

[1]*Chair of Computational Mechanics, Université de Technologie Compiègne, Compiègne, France*
[2]*Faculty of Civil Engineering, University of Sarajevo, Sarajevo, BiH*
[3]*Institut Universitaire de France, Paris, France*
[4]*Université de Technologie Compiègne, LMAC, Compiègne, France*

(Received January 31, 2022, Revised February 8, 2022, Accepted February 9, 2022)

Abstract. In this paper we deal with classical instability problems of heterogeneous Euler beam under conservative loading. It is chosen as the model problem to systematically present several possible solution methods from simplest deterministic to more complex stochastic approach, both of which that can handle more complex engineering problems. We first present classical analytic solution along with rigorous definition of the classical Euler buckling problem starting from homogeneous beam with either simplified linearized theory or the most general geometrically exact beam theory. We then present the numerical solution to this problem by using reduced model constructed by discrete approximation based upon the weak form of the instability problem featuring von Karman (virtual) strain combined with the finite element method. We explain how such numerical approach can easily be adapted to solving instability problems much more complex than classical Euler's beam and in particular for heterogeneous beam, where analytic solution is not readily available. We finally present the stochastic approach making use of the Duffing oscillator, as the corresponding reduced model for heterogeneous Euler's beam within the dynamics framework. We show that such an approach allows computing probability density function quantifying all possible solutions to this instability problem. We conclude that increased computational cost of the stochastic framework is more than compensated by its ability to take into account beam material heterogeneities described in terms of fast oscillating stochastic process, which is typical of time evolution of internal variables describing plasticity and damage.

Keywords: duffing oscillator; Euler beam; instability problem; stochastic approach; von Karman strain

1. Introduction

The classical problem of Euler instability, dealing with the bifurcation of an inextensible beam with zero shear deformation, is the basis of any traditional instability course in engineering curricula. Typical studies in many textbooks (Timoshenko and Gere 1961) cover how to obtain a simple analytic solution for critical equilibrium state by solving the strong form of governing equilibrium equation in deformed beam configuration. This is possible to achieve for a linear elastic homogeneous beam and a chosen set of elementary boundary conditions, such as simply supported or built-in beams, concluding that the exact deformed shape corresponds to either *sin* or

*Corresponding author, Professor, E-mail: adnan.ibrahimbegovic@utc.fr

Copyright © 2022 Techno-Press, Ltd.
http://www.techno-press.org/?journal=csm&subpage=8 ISSN: 2234-2184 (Print), 2234-2192 (Online)

cos function verifying all governing equations (kinematics, constitutive and equilibrium) in each and every point of deformed configuration. The solution to more complex (heterogeneous) structures, can no longer be computed with analytic approach. Similarly, presenting an analytic solution for Euler's cantilever beam under compressive force that goes beyond the critical bifurcation loading, is only provided for free-end displacements and rotations (Timoshenko and Gere 1961).

Therefore, the practicing engineers facing the instability problems of more complex (heterogeneous) structures are stranded with the question on how to reduce solving the real problem at hands to Euler beam solution. Examples of this kind are numerous, from a complex structure geometry that cannot be approximated by beam to those built of heterogeneous engineering materials. These are the kind of issues we seek to address in this paper on the basis of chosen model of Euler beam instability.

More precisely, we construct the reduced numerical models for solving this problem that deliver discrete approximation to computed solution that can be adapted to any structure complexity, which can be made as precise as needed with an increase in computational cost. In particular, we first illustrate the reduced model constructed from the weak form of the problem featuring von Karman virtual strain and discrete approximation based upon the finite element method (Ibrahimbegovic 2009). This approach follows in the footsteps of our previous works, e.g., (Ibrahimbegovic *et al.* 2013, Medic *et al.* 2013, Hajdo, *et al.* 2020, Mejia-Nava, *et al.* 2020), but extended to the case where the beam material need not be homogeneous, but highly heterogeneous. For validating the proposed approach against the classical Euler solution, we choose the problem with the beam material properties varying as fast-oscillating periodic function, which can also be solved by homogenization (Ibrahimbegovic 2009).

We show that the same kind of reduced model can also be constructed for the geometrically exact beam, the model that has been developed for representing large displacement and rotations of the beam; e.g., see (Ibrahimbegovic 1995, Ibrahimbegovic 1997, Ibrahimbegovic and AlMikdad 1998, Ibrahimbegovic and Taylor 2002). Such a beam model can easily be adapted to non-homogeneous elastic or even inelastic beam behavior, as already shown in (Dujc *et al.* 2010) or (Imamovic *et al.* 2019). Hence, here we restrict our analysis to providing the complete solution for deformed configuration of a cantilever beam under the load that goes beyond the critical value of bifurcation force.

The final reduced model for the Euler instability problem is constructed within the stochastic framework by making use of Duffing oscillator. Such a reduced model for the Euler instability is developed within the dynamics framework, where instability can be represented in terms of Lyapunov criterion (Lozano *et al.* 2000) by using the corresponding Hamiltonian as the total energy of the vibrating beam. In order to control vibrations, we also add linear damping term, combined with nonlinear (cubic approximation) to elastic force leading to chaotic vibrations that ought to be studied in the most appropriate stochastic framework, e.g., see (Arnold 1974, Cai and Lin 1988, Kree and Soize 2012, Guckenheimer and Holmes 2013). We further seek to provide the estimate of the beam (nonlinear) response under white noise excitation, which can be obtained by using the standard tools for stochastic differential equations, e.g., see (Ethier and Kurtz 2009, Khasminskii 2011, Liptser and Shiryayev 2012).

All these developments, which have been carried out for conservative loads, can easily be extended to non-conservative loads by following the works in (Hajdo *et al.* 2021, Masjedi and Ovesy 2015, Gasparini *et al.* 1995, Culver *et al.* 2019), but with an adequate selection of damping phenomena (Ibrahimbegovic *et al*. 2021, Mejia-Nava *et al.* 2022).

The paper outline is as follows. In Section 2, we present two alternative formulations for the Euler instability problem, starting for linearized or nonlinear formulation combined with the consistent linearization. We then briefly recall the analytic solution for each in Section 3. Numerical solutions for reduced model are constructed in Section 4, both in terms of the weak form with von Karman virtual strain and in terms of Duffing oscillator. In Section 5, we present different methods for Duffing oscillator under either fast periodic loading or under white noise signal. Conclusions are drawn in Section 6.

2. Euler instability problem: two alternative formulations

In this section we briefly discuss two alternative formulations of the Euler instability problem. One such formulation starts with linearized formulation of kinematics and constitutive equations, combined with nonlinear equilibrium equation established in the deformed configuration of the beam (e.g., see Ibrahimbegovic 2009). An alternative theoretical formulation within geometrically exact framework considers instability of a compressed cantilever beam under fixed force (e.g., see Ibrahimbegovic 1995, Ibrahimbegovic 1997), and carries out consistent linearization in order to derive the corresponding strong form of instability problem for Euler beam.

2.1 Linearized instability approach to Euler buckling

The first theoretical formulation is based upon strong form of Euler beam, verifying the equations of kinematics, constitutive law and equilibrium. The beam material behavior is considered linear elastic (characterized by Young's modulus E). In the deformed configuration of the beam, we have no change of thickness and enforce that the cross-section remains orthogonal with respect to the beam neutral axis. The first two equations are borrowed from linearized beam theory. Namely, with $u(x)$ and $v(x)$ denoting horizontal and vertical displacement of the point in the chosen cross section which does not have any bending deformation (e.g., beam neutral axis; see Fig. 1), we can write these linear kinematic and constitutive equations as follows:

1. Kinematics (see Fig. 1(b))

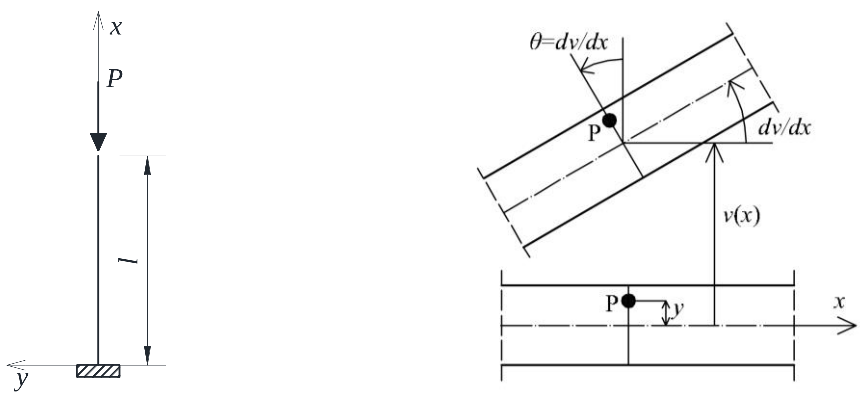

(a) Euler cantilever beam - global configuration (b) Initial and deformed beam axis

Fig. 1 Classical linearized instability of Euler cantilever beam

$$\left.\begin{aligned} u^p(x,y) &:= -y\cdot\theta = -y\frac{dv(x)}{dx} \\ v^p(x,y) &= v(x) \end{aligned}\right\} \Rightarrow \varepsilon^p_{xx}(x,y) := \frac{du^p}{dx} = -y\frac{d^2v^p}{dx^2} \tag{1}$$

2. Constitutive law

$$\begin{aligned} \sigma_{xx}(x,y) &:= E\varepsilon_{xx}(x,y) = -Ey\frac{d^2v^p}{dx^2} \\ M &:= -\int_A y\sigma_{xx}dA = E\frac{bh^3}{12}\frac{d^2v(x)}{dx^2} = EI\frac{d^2v(x)}{dx^2} \end{aligned} \tag{2}$$

where b and h are respectively the width and the height of rectangular cross section (chosen for illustration), M is a bending moment, E modulus of elasticity and I is a moment of inertia.

However, the third equation takes into account nonlinearity, seeking to establish equilibrium in the beam deformed configuration:

3. Equilibrium

$$\begin{aligned} 0 &= \sum F_y := \frac{dT(x)}{dx} + q(x) \\ 0 &= \sum M := \frac{dM(x)}{dx} + T(x) + P\frac{dv}{dx} \end{aligned} \tag{3}$$

were T is a shear force and q is a transverse distributed load. These three equations can be combined within a single equilibrium equation expressed in terms of displacement, so called strong form of the Euler beam instability problem

$$\frac{d^4v(x)}{dx^4} + \frac{P}{EI}\frac{d^2v(x)}{dx^2} = \frac{q(x)}{EI} \tag{4}$$

By assuming zero transverse loading, q=0, we obtain the final strong form of the problem

$$\frac{d^4v(x)}{dx^4} + k^2\frac{d^2v(x)}{dx^2} = 0 \quad ; \quad k = \sqrt{\frac{P}{EI}} \tag{5}$$

2.2 Nonlinear instability of Euler beam and its consistent linearization

If we now turn to geometrically exact framework, by using large displacements and rotations, one can picture the deformed configuration of the beam as depicted in Fig. 2.

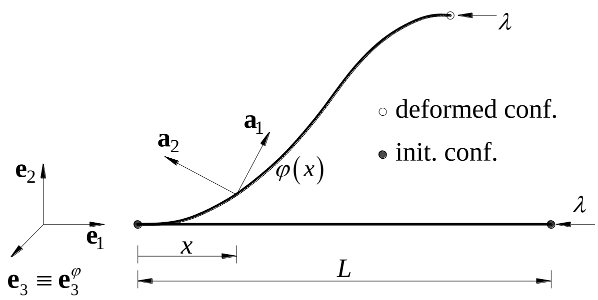

Fig. 2 Nonlinear instability of geometrically exact Euler cantilever beam

In development of governing equations for Euler instability problem, here we will follow an original approach by using Reissner's geometrically exact beam model (see Ibrahimbegovic 1995, 1997, Ibrahimbegovic and AlMikdad 1998, Ibrahimbegovic and Taylor 2002), where each particle in the deformed configuration can be described by position vector, that can be written by using (large) displacements vector components *u* and *v* leading to:

$$\varphi = (x+u)\boldsymbol{e}_1 + v\boldsymbol{e}_2.$$

Reissner's beam model hypothesis is somewhat more general than the one of Euler's beam, assuming that the cross section remains plane (and non-deformable), but not necessarily orthogonal to the beam deformed axis. This implies that we can obtain a new position of unit vector $\mathbf{a}_i$, which remains orthogonal to cross-section (but not tangent to beam axis), simply by a large rotation of its initial position (here aligned with coordinate axis $\mathbf{e}_i$). This can be written by using an orthogonal matrix $\boldsymbol{\Lambda}$ with $\mathbf{a}_i = \boldsymbol{\Lambda}\ \mathbf{e}_i$. In 2D the orthogonal matrix components can be defined in terms of (large) rotation angle θ

$$\boldsymbol{a}_i = \boldsymbol{\Lambda}\boldsymbol{e}_i\ ;\ \boldsymbol{\Lambda} = \begin{bmatrix} \cos\theta & -\sin\theta & 0 \\ \sin\theta & \cos\theta & 0 \\ 0 & 0 & 1 \end{bmatrix} \Leftrightarrow \begin{array}{l} \boldsymbol{a}_1 = \cos\theta\,\boldsymbol{e}_1 + \sin\theta\,\boldsymbol{e}_2 \\ \boldsymbol{a}_2 = -\sin\theta\,\boldsymbol{e}_1 + \cos\theta\,\boldsymbol{e}_2 \\ \boldsymbol{a}_3 = \boldsymbol{e}_3 \end{array} \tag{6}$$

We can further define the finite strain measure (Ibrahimbegovic and Taylor 2002) both for axial strain E and shear strain Γ

$$\begin{array}{c} E = a_1^T\varphi' - e_1^T e_1 \ \Rightarrow\ a_1^T\varphi' = E + 1 \\ \Gamma = a_2^T\varphi' - e_2^T e_1 \ \Rightarrow\ a_2^T\varphi' = \Gamma \end{array} \tag{7}$$

where φ' is the derivative of position vector. Since the local frame in the deformed configuration is still an orthogonal frame, we can write the derivative of position vector as

$$\boldsymbol{\varphi}' = (1+E)\mathbf{a}_1 + \Gamma\mathbf{a}_2$$

Moreover, given that we have statically determined problem, we can also obtain the force equilibrium equation by decomposing the applied force within the same local orthogonal frame in deformed configuration

$$n = N\boldsymbol{a}_1 + V\boldsymbol{a}_2 \Rightarrow \begin{array}{l} N = -\lambda\cos\theta \\ V = \lambda\sin\theta \end{array} \tag{8}$$

thus defining normal force component *N* and shear force component *V*. Furthermore, by replacing the last two results into the moment equilibrium equation, we can write

$$\begin{aligned} 0 &= m' + \varphi' \times \mathbf{n} \qquad \left| m = (EI)\theta' \right. \\ &= (EI)\theta'' + \lambda\left[(1+E)\sin\theta + \Gamma\cos\theta\right] \end{aligned} \tag{9}$$

For classical Euler's beam, yet called Euler's *elastica*, we assume that both shear and axial strain components are equal to zero, which leads to (nonlinear) equilibrium equation in deformed configuration defined in terms of angle θ:

$$\Gamma = 0 \ \text{ and } E = 0 \Rightarrow\ EI\theta'' + \lambda\, sin\,\theta = 0$$

The corresponding linearized form or Euler instability, referred to as Euler buckling, can be recovered from the last result by enforcing a small pre-buckling displacement with

$$sin\,\theta \approx \theta \Rightarrow EI\theta'' + \lambda\theta = 0$$

By further using that $\theta = \frac{dv}{dx}$ and λ=P, we recover the same result for the strong form of Euler instability problem as already defined in (5).

3. Analytic solution based on strong form

3.1 Euler buckling load solution

In this section we briefly discuss the analytic solutions for instability of the classic problem of linearized instability of a homogeneous cantilever under fixed compressive force. The analytic solution satisfying all three fundamental equations combined within the strong form of Euler instability problem, stated in (5).

$$\frac{d^4v(x)}{dx^4} + k^2\frac{d^2v(x)}{dx^2} = 0 \quad ; \quad k = \sqrt{\frac{P}{EI}} \tag{10}$$

The general solution for such equation can be written as

$$v(x) = A_1 \sin k\,x + A_2 \cos k\,x + A_3 x + A_4 \tag{11}$$

where A_1, A_2, A_3 and A_4 are constants to be obtained from boundary conditions. For cantilever beam in Fig. 1, we can readily conclude that the boundary conditions can be written as

$$v(0) = 0 \quad ; \quad \frac{dv(0)}{dx} = 0 \quad ; \quad M(l) = EI\frac{d^2v(l)}{dx^2} = 0\,; \quad T(l) = -EI\frac{d^3v(l)}{dx^3} - P\frac{dv(l)}{dx} = 0 \tag{12}$$

By combining results in Eqs. (11) and (12), we can obtain:

$$|\Rightarrow \underbrace{\begin{bmatrix} 0 & 1 & 0 & 1 \\ k & 0 & 1 & 0 \\ -k^2 \sin k\,l & -k^2 \cos k\,l & 0 & 0 \\ 0 & 0 & k^2 & 0 \end{bmatrix}}_{det[\bullet]=0} \begin{bmatrix} A_1 \\ A_2 \\ A_3 \\ A_4 \end{bmatrix} = \begin{bmatrix} 0 \\ 0 \\ 0 \\ 0 \end{bmatrix}$$

From the above condition of zero determinant which guarantee non-trivial solution, it follows that:

$$k^2 \cos k\,l = 0 \quad \Rightarrow \quad \cos k\,l = 0 \quad \Rightarrow \quad kl = \frac{2n-1}{2}\pi \;\; , \;\; n = 1,2,\ldots$$

If we recall the relation k^2=P/EI given in Eq. (10), we further get solution for (all) applied load values that provide non-trivial solutions and corresponding deformed configuration modes:

$$P_n = \frac{(2n-1)^2\pi^2 EI}{4l^2}\,; \Phi_n(x) = -\cos\frac{(2n-1)\pi x}{2l} + 1$$

The critical force for buckling of Euler's cantilever beam is to the smallest load value:

$$P_{cr} = \frac{\pi^2 EI}{(2l)^2}$$

and the corresponding buckling mode is:

$$\Phi_1(x) = 1 - \cos\frac{\pi x}{2l}$$

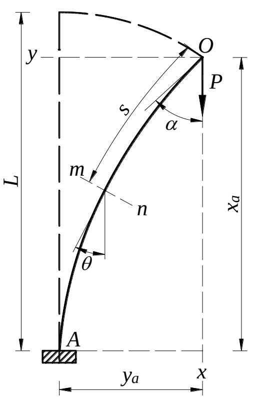

Fig. 3(a) Geometrically exact Euler beam under compressive fixed load-geometry and load

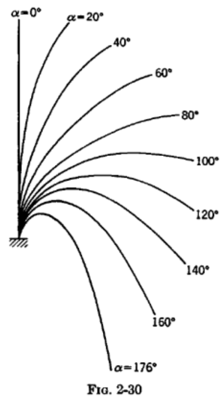

Fig. 3(b) Geometrically exact Euler beam under compressive fixed load-deformed shapes

Table 1 Load-deflection data for a buckled bar

α	0°	20°	40°	60°	80°	100°	120°	140°	160°	176°
$\frac{P}{P_{cr}}$	1	1.015	1.063	1.152	1.293	1.518	1.884	2.541	4.029	9.116
$\frac{x_a}{l}$	1	0.970	0.881	0.741	0.560	0.349	0.123	-0.107	-0.340	-0.577
$\frac{y_a}{l}$	0	0.220	0.422	0.593	0.719	0.792	0.803	0.750	0.625	0.421

3.2 Nonlinear instability response for geometrically exact beam

In this section we only present the analytic solution results presented in (Timoshenko and Gere 1961), for instability of the geometrically exact homogeneous cantilever under fixed compressive force (see Fig. 3(a)). The model of this kind allows that the computations can carry on after bifurcation point, followed by very large displacements and rotations (see Fig. 3(b)).

In Table 1 we only present the analytic solution results presented in (Timoshenko and Gere 1961), for free-end displacement components that confirm the ability of geometrically exact beam model to represent very large displacements and rotations. The same results have been confirmed numerically for chosen beam properties: cross-section A=1 [cm^2], moment of inertia I=0.006 [cm^4], length l=100 [cm] and Young's modulus E=10^6 [N/cm^2] in (Mejia-Nava *et al.* 2022) by using the geometrically exact beam model in (Imamovic and Ibrahimbegovic, Hajdo 2019).

4. Numerical solution based on reduced models with finite element method

In this section we will show how numerical framework can be generalized to more complex problems that can be solved by using reduced models constructed with the finite element method. In constructing the weak form solution, the key role is played by von Karman type of strain measure. In our previous work (Ibrahimbegovic *et al*. 2013, Hajdo *et al*. 2020), the von Karman strain was used for formulating instability problems as linear buckling analysis of truss structures, which reduces to solving the linear eigenvalue problem. Here, we carry on further to introduce the

Euler-Bernoulli beam with the von Karman strain measure, as the model capable of accounting for geometric nonlinearities. We will also add the special finite element that can take into account the follower force as the source of instability.

4.1 Euler beam element with linearized kinematics and von Karman virtual strain

If we consider for example an axially compressed beam, the strong form of the problem can be written for the case of small deformations and moderate rotations as

$$\frac{d^4 v}{dx^4} + \frac{P}{EI}\frac{d^2 v}{dx^2} = 0 \tag{12}$$

where *v* is transverse displacement, *P* is compressive force, *E* is Young's modulus and *I* is moment of inertia of beam's cross section. By solving this differential equation, we obtain the Euler critical buckling force. Unfortunately, such a result can only be obtained for simple problems; if one wants to solve more complex problems, we have to employ the weak form, or virtual work (e.g., Ibrahimbegovic 2009). The key role here is played by virtual von Karman strain constructed under hypothesis that deformations are small and rotations are moderate. Under such hypothesis the von Karman deformation measure can be defined for the Euler-Bernoulli beam as follows

$$\varepsilon^{vK} = \frac{du}{dx} + \frac{1}{2}\left(\frac{dv}{dx}\right)^2 - y\frac{d^2 v}{dx^2} \tag{13}$$

By introducing virtual displacements $(\hat{u}, \hat{v})$ to produce the perturbed configuration of the beam deformed configuration, we can apply the Gâteaux derivative in the direction of these virtual displacements to obtain the virtual von Karman deformation

$$\hat{\varepsilon}^{vK} = \frac{d\hat{u}}{dx} + \frac{dv}{dx}\frac{d\hat{v}}{dx} - y\frac{d^2\hat{v}}{dx^2} \tag{14}$$

With this result in hand we can further write the virtual work of internal forces

$$\delta\Pi \int_l \int_A \hat{\varepsilon}^{vK} \sigma dA dx \int_l \left(\frac{d\hat{u}}{dx}N + \frac{d^2\hat{v}}{dx^2}M\right)dx \int_l \frac{d\hat{v}}{dx}\frac{dv}{dx}N dx_{\;int} \tag{15}$$

The beam stress resultants in terms of axial force *N* and bending moment *M* are given as

$$N(x) = EA\frac{du}{dx} \quad ; \quad M(x) = EI\frac{d^2 v}{dx^2} \tag{16}$$

We note that the values of stress resultants *N* and *M* are obtained from linear theory. Further, we can write an explicit form of the principle of the virtual work or the variational equation

$$\int_l \frac{d\hat{u}}{dx} EA \frac{du}{dx} dx + \int_l \frac{d^2\hat{v}}{dx^2} EI \frac{d^2 v}{dx^2} dx + \int_l \frac{d\hat{v}}{dx}\frac{dv}{dx} N dx = \hat{u} f^{ext} \tag{17}$$

where f^{ext} is an external force. The latter is the basis for the approximate solution of instability problem, which can be obtained by the finite element method (Ibrahimbegovic 2009), for a structure of arbitrary complexity.

To define the finite element approximation discrete approximation, we will use a two-node Euler-Bernoulli beam element. In 2D case, each node has three degrees of freedom, two translations and one rotation. The nodal values of the real and virtual displacements are denoted as

$$d = [u_1 \quad v_1 \quad \varphi_1 \quad u_2 \quad v_2 \quad \varphi_2]$$
$$\hat{d} = [\hat{u}_1 \quad \hat{v}_1 \quad \hat{\varphi}_1 \quad \hat{u}_2 \quad \hat{v}_2 \quad \hat{\varphi}_2] \tag{18}$$

The real displacement field interpolation is given as

$$u(x) = N_1(x)u_1 + N_2(x)u_2$$
$$v(x) = H_1(x)v_1 + H_2(x)\varphi_1 + H_3(x)v_2 + H_4(x)\varphi_4 \tag{19}$$

In Eq. (19) above, N_i are the linear shape functions, and H_j are the Hermite cubic polynomials

$$N_1(x) = 1 - \frac{x}{l} \qquad N_2(x) = \frac{x}{l}$$
$$H_1(x) = 1 - 3\left(\frac{x}{l}\right)^2 + 2\left(\frac{x}{l}\right)^3 \qquad H_2(x) = x - 2\frac{x^2}{l} + \frac{x^3}{l^2} \tag{20}$$
$$H_3(x) = 3\left(\frac{x}{l}\right)^2 - 2\left(\frac{x}{l}\right)^3 \qquad H_4(x) = -\frac{x^2}{l} + \frac{x^3}{l^2}$$

where l is the length of the beam element. The same kind of interpolation given in Eq. (19) is chosen for the virtual displacement field. The derivatives of the shape functions, and the corresponding axial deformations can then easily be obtained as follows

$$\frac{du}{dx}(x) = \sum_{a=1}^{2} \frac{dN_a}{dx} u_a = \bar{N}d \quad ; \quad \frac{d\hat{u}}{dx}(x) = \hat{d}^T \bar{N}^T \quad ; \bar{\mathrm{N}} = \begin{bmatrix} \frac{dN_1}{dx} & 0 & 0 & \frac{dN_2}{dx} & 0 & 0 \end{bmatrix} \tag{21}$$

We can further obtain the first derivatives of the transverse displacement

$$\frac{dv}{dx}(x) = \bar{H}d \quad ; \quad \frac{d\hat{v}}{dx}(x) = \hat{d}^T \bar{H}^T \quad ; \bar{\mathrm{H}} = \begin{bmatrix} 0 & \frac{dH_1}{dx} & \frac{dH_2}{dx} & 0 & \frac{dH_3}{dx} & \frac{dH_4}{dx} \end{bmatrix} \tag{22}$$

and furthermore the bending strains as its second derivative

$$\frac{d^2v}{dx^2}(x) = Bd \quad ; \quad \frac{d^2\hat{v}}{dx^2}(x) = \hat{d}^T B^T \quad ; \mathrm{B} = \begin{bmatrix} 0 & \frac{d^2H_1}{dx^2} & \frac{d^2H_2}{dx^2} & 0 & \frac{d^2H_3}{dx^2} & \frac{d^2H_4}{dx^2} \end{bmatrix} \tag{24}$$

By replacing these results into the relation given in Eq. (17), we can finally obtain the beam element internal force vector

$$\hat{\mathbf{d}}^T f^{\mathrm{int}} = \hat{\mathbf{d}}^T \underbrace{\int_l \left(\bar{\mathbf{N}}^T EA\bar{\mathbf{N}} + \mathbf{B}^T EI\mathbf{B}\right) dx}_{\mathbf{K}_m} \mathbf{d} + \hat{\mathbf{d}}^T \underbrace{\int_l \bar{\mathbf{H}}^T \bar{\mathbf{H}} N dx}_{\mathbf{K}_g} \mathbf{d} \tag{24}$$

where E elasticity modulus, A is the cross-section area, I moment of inertia, l is element length, and N axial force. The same discrete approximation with finite elements allows defining the beam element tangent stiffness matrix

$$K_t = K_m + K_g \;;$$
$$K_m = \int_l (\bar{N}^T EA\bar{N} + B^T EIB) dx \quad ; \quad \mathrm{K}_g = \int_l \bar{H}^T \bar{H} N dx \tag{25}$$

We note that the tangent stiffness matrix consists of material and geometric parts. We also note that axial internal force N in (47) above is computed by linearized kinematics, which implies that the geometric stiffness is linearly proportional to external loads. Hence, we can reformulate the external loading as product of load multiplier (denoted as P) and reference (typically unit) value of applied loads $\bar{\imath}$ (producing axial internal force n), writing $f^{\mathrm{ext}}=P\,\bar{\imath}$, which allows to recast tangent stiffness indicated linearity of geometric stiffness with respect to load multiplier

$$K_t = K_m + PK_G \;\; ; \quad \mathrm{K}_G = \int_l \bar{H}^T \bar{H} n dx \tag{26}$$

The instability criterion can then be formulated as the singularity of the tangent stiffness matrix, with corresponding eigenvalue equal to zero

$$[K_m + PK_G]\phi = 0 \;\; \Rightarrow \;\; \mathrm{P}_{cr,}\phi_{cr}$$

where $\mathrm{P}_{cr,}\phi_{cr}$ are the corresponding critical buckling load multiplier and critical mode of instability. The last results clearly illustrated that instability is produced with compressive loads. The computations of the buckling load can be solved by standard methods for linear eigenvalue problem (Parlett 1980), very much similar to methods used in dynamics for computing natural frequencies (Clough 2006).

4.2 Heterogeneous Euler beam buckling computations

Here we give a numerical example of a heterogeneous beam. In these computations we keep previously described Euler beam element with linearized kinematics and von Karman virtual strain to obtain the weak form governing equations. However, the constitutive model is now different. Namely, we here study the Euler buckling or linearized instability with fast varying Young's modulus

$$E(x) = E\left[1 - 0.05 \sin\left(n\frac{2\pi x}{l}\right)\right]; \quad l_i = \frac{l}{n}$$

where n is number of finite elements along the beam, and l_i is the corresponding length of each element if such finite element mesh. This choice is made for simplifying the beam material data preparation that allows representing Young's modulus $E(x)$ with point values in the center of each element, which further reduces to two different materials when modeling the beam. Hence, a simple homogenization procedure (Ibrahimbegovic 2009) under constant axial stress can easily provide the average value of Young's modulus.

We note that the cross section is constant along the beam. Thus, geometric and material properties of the beam chosen for computations are given in Table 2. The first material with Young's modulus E_1=0.95E, while for the second material we choose E_2=1.05E. We perform several computations for different number of elements (n=2; 10; 20; 100; 200 and 2000). In each computation, the Young's modulus E_1 is associated with any odd number element, while E_2 is attributed to any even number element.

Table 2 Geometric and material properties of a beam

A [cm^2]	I [cm^4]	l [cm]	E [N/cm^2]	E_1=0.95E	E_2=1.05E
1.0	0.006	100	10^6	950000	1050000

Table 3 Critical force values using oscillating values of Young's modulus (E_1 for odd and E_2 for even number of element)

n	2	10	20	100	200	2000
F_{cr} [N]	1.587	1.475	1.475	1.476	1.476	1.477

Table 4 Critical force values using constant average Young's modulus, even numbers

n	2	10	20	100	200	2000
F_{cr} $[N]$	1.643	1.483	1.478	1.477	1.477	1.477

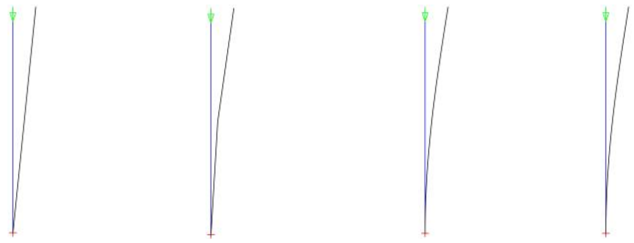

n=1 n=2 n=20 n=2000

Fig. 4 The first buckling mode for different meshes

The obtained values for critical force, obtained by using Euler's beam and eigenvalue problem computations, are given in Table 3.

In Table 4 are given results of computations for critical force performed with average value of Young's modulus. The average Young's modulus E is obtained by homogenization with respect to constant axial force (constant stress σ): $\sigma E^{-1}\sigma l = \sum_{i=1}^{n} \sigma E_i^{-1} \sigma l_i \quad \Rightarrow \quad E^{-1} l = \sum_{i=1}^{n} E_i^{-1} l_i$, where n is number of elements, and l_i is length of the element. In case of even number of elements given, the average value of Young's modulus is E = 997500 N/cm^2.

From the previously presented results we can conclude that if we have a sufficiently refined mesh, the computation with the average value of Young's modulus obtained by homogenization (Ibrahimbegovic 2009) will result in the same value of critical force as the computation performed with different value of Young's modulus along the beam. In other words homogenization of beam material properties and computations with refining the finite element mesh will lead us to the same results. However, if the beam heterogeneities are more pronounced, which corresponds to large initial (or induced) defects or to computing with a coarse finite element mesh, the results are no longer the same. Moreover, the true value of critical load is lower for real heterogeneous beam material, which is in agreement that the initial (or induced) defects can trigger pre-mature instability. Hence, the overall comprehensive results regarding the role of heterogeneities (or defects) can only be obtained by using the stochastic approach, which is discussed in the second part of this paper.

The first buckling mode computed for several different choices for the finite element mesh with rather different number of elements is given in Fig. 4, showing that the critical mode is less affected, which is typical of linearized instability. This is no longer the case for instability of geometrically exact beam (Mejia-Nava *et al*. 2022).

4.3 Reduced model simulation of Euler instability via Duffing oscillator

In this section we revisit the instability problem defined by Euler, but presented within the dynamics framework in terms of reduced model of Duffing oscillator (Guckenheimer and Holmes 2013). The model reduction is carried out by using the finite element discrete approximation featuring 0D problem formulation defined in terms of a nonlinear ordinary differential equation in

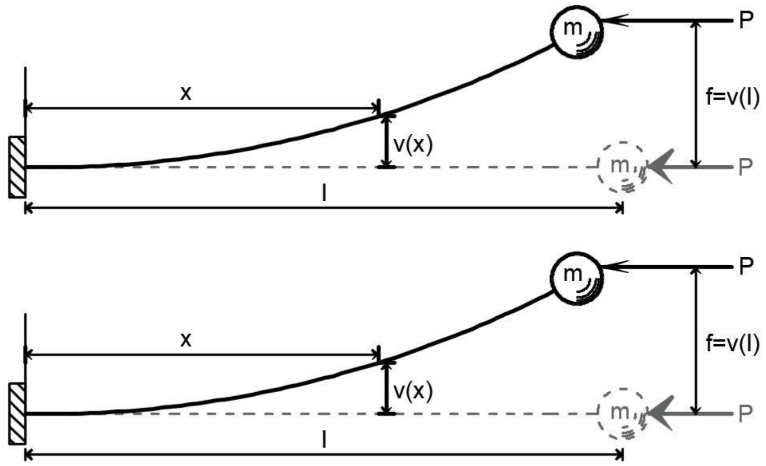

Fig. 5 Euler-Bernoulli cantilever beam vibrations under fixed load ($v(x,t)$ $Px=P$, $Py=0$)

time, with cubic nonlinearity. Here, we consider a cantilever beam of length l to which we apply at its free end a compression force $\lambda=P$ (see Fig. 5).

By denoting by $\theta(x)$ the angle between the cross section and the neutral axis at any point $x\in[0,l]$ in beam initial configuration, we can obtain the geometrically exact equilibrium equation on beam deformed axis (as already explained in Section 2) that reads

$$EI\frac{d^2\theta(x)}{dx^2}+\lambda\sin\big(\theta(x)\big)=0 \tag{27}$$

where Young's modulus E and cross-section inertia I are assumed to be constant, for the moment. For critical force λ_{cr}, this equilibrium is unstable, with any small perturbation that can produce disproportional response leading to very large displacements rotations, where geometrically exact beam formulation (e.g., Ibrahimbegovic 1995, Ibrahimbegovic 1997, Ibrahimbegovic and Taylor 2002) can be used (for simplified computations of beam deformed axis, we refer to (Timoshenko 1980).

Let us now reconsider the problem within dynamics framework, which can be obtained by adding the inertia term that takes a linear form due to using the Lagrangian formulation

$$m\frac{d^2\theta(x,\ t)}{dt^2}-EI\frac{d^2\theta(x,\ t)}{dx^2}-\lambda\sin[\theta(x,\ t)]=0 \tag{28}$$

where m denotes the lumped beam mass. We note that $\theta(x,t)$ in dynamics setting is a function of both space x and time t.

In order to simplify such dynamics framework, we will further replace sin-function by asymptotic development truncated after cubic term resulting with: $\sin[\theta]=\theta-\theta^3/3!$

$$m\frac{d^2\theta(x,t)}{dt^2}-EI\frac{d^2\theta(x,t)}{dx^2}-\lambda\left[\theta(x,t)-\frac{\theta^3(x,t)}{3!}\right]=\widehat{W}(t) \tag{29}$$

In (3) above we also add a temporal white noise solicitation $\hat{W}$ when extending to stochastic framework. Note that $\hat{W}$ can be interpreted as the time derivative of a standard Wiener process W only in the sense of the distributions, since a Wiener process is not diffrentiable. We also note that the chosen white noise is only in time $\hat{W}(t)$, which means that the external stochastic compressive force remains constant along the beam at any given time. We could have considered a space-time white noise but it would have changed a bit the step of averaging over space dimension *x*. The exact details about this time white noise, its interpretability and its 'homogeneity' with respect to the other terms of the equation are still to be explained.

Finally, by adding a viscous damping term (Ibrahimbegovic and Mejia-Nava 2021) proportional to viscosity coefficient δ, we get the final form of beam equation of motion in forced vibrations

$$m\frac{d^2\theta(x,\ t)}{dt^2}+\delta\frac{d\theta(x,\ t)}{dt}-EI\frac{d^2\theta(x,\ t)}{dx^2}+\ \lambda\frac{\theta^3(x,\ t)}{6}\ -\lambda\,\theta(x,\ t)=\widehat{W}(t) \tag{30}$$

In order to provide reduced model for such forced vibrations case that will allow providing analytic solution, we proceed with the method of separation of variables. Namely, we suppose that $\theta(x,\ t)$ can be written as a product of two functions, one depending only on space and other on time, $\theta(x,\ t)=H(x)Y(t)$. This separation of variables can be seen as the decomposition of the solution in terms a shape functions dependent on *x*, expressed as the solution of a static equilibrium for the beam, which allows reusing the Hermite polynomials $H(x)$, as already defined in (20), multiplied by a time evolution function that modulate such shape function.

Hence, we conclude that motion described herein corresponds to stationary waves phenomena. This kind of hyperbolic partial diffrential equation, contrary to a progressive wave phenomenon, can be tackled by the separation of variables approach. Note that the space stationarity of the wave propagation is crucial for justification of chosen approach. Namely, the stationary wave can be represented as $v(x,t)=H(x)\ \sin(vt)$, whereas the progressive waves is rather represented as $v(x,t)=S\ \sin(vt-x)$. We note that the first is separable, but the second is not.

With such an expression for θ, we further obtain (denoting the time derivative with superposed dot)

$$mH(x)\ddot{Y}(t)+\delta H(x)\dot{Y}(t)+\frac{\lambda}{6}H^3(x)H^3(t)-[EI+\lambda]H(x)Y(t)=\hat{W} \tag{31}$$

If now we integrate over $x\in[0,l]$, it only remains an ordinary differential equation of the time variable *t*. This integration over *x* can be seen as a spatial averaging operation. By this we mean that instead of considering the beam as a continuum of points, we decide to consider the beam as a single point system. So, concerning the space variable, we go from a 1D model to a 0D model. Then, instead of considering forces as function of space and time, we have to consider the resultant of each kind of force only as a function of time and, so, averaged in space. For example, the inertial force, here described by a space-time function, has to be space averaged to give $\int_l m\,H(x)Y(t)dx=m\int_l\ H(x)dx\ \ Y(t)$. Doing this for each term, we obtain a reduced equation dependent only on time. This method is not necessarily good, and this averaging obviously leads to a great loss of information but, on the other hand, it simplifies things hugely and makes possible to work on a point reduced approximate system

$$mA\ \ddot{Y}t+\ \delta A\ Yt\ +\ \lambda 6\ B\ Y3t\ –EIC\ +\ \lambda AYt=lWt \tag{32}$$

where *A*, *B* and *C* are constants depending on the chosen shape function *S* that can be expressed as follows

$$A=lH(x)dx\ ;\ B=lH'(x)dx\ ;\ C=lH''(x)\ dx \tag{33}$$

Finally, by dividing by mA, we can express the result in (6) in the format of the Duffing equation, with a white noise solicitation

$$\ddot{Y}(t) + \left[\frac{\delta}{m}\right] \dot{Y}(t) + \left[\frac{\lambda B}{6mA}\right] Y^3(t) - [EIC/mA + \lambda/m]Y(t) = (l/\,mA)\widehat{W}(t) \tag{34}$$

In summary, the Duffing equation represents dynamic oscillation of reduced model, which consists of mass-dashpot-spring system, where the elastic spring stiffness is nonlinear (cubic) function of vibration amplitude.

We will first study such an equation in the forced vibration regime, brought by applying harmonic load instead of white noise, and recast by using a simplified notation in the following format

$$\ddot{x} + \delta\dot{x} + \alpha x^3 + \beta x = \gamma \cos(\omega t) \tag{35}$$

where by hypothesis it holds that $\delta>0$, $\alpha>0$. The nonlinear spring can also be characterized by the following elastic potential $V(x)=\alpha\, x^4/4+\beta\, x^2/2$.

The case when $\gamma=0$ represents the free vibrations of the reduced model. In such a case, the system admits one (stable) equilibrium state if $\beta<0$ or three equilibrium states (with only two of them stable) if $\beta>0$. The number of stable equilibrium states can be observed from corresponding form of elastic potential that depends on sign of β, which is either positive or negative for a force smaller or larger than critical force.

An alternative way to present this equation is in phase space in terms of autonomous system of the first order differential equations

$$\begin{aligned} \dot{u} &= v \\ \dot{v} &= -\delta v - \alpha u^3 - \beta u \end{aligned} \tag{36}$$

The set of format, for the case non-damped case with $\delta=0$, allows us to provide the corresponding Hamiltonian as the total energy of the system, as the sum of kinetic energy $U=u^2/2$ and potential energy $V=\alpha\, x^4/4+\beta\, x^2/2$

$$H := U + V = \frac{u^2}{2} + \alpha\frac{x^4}{4} + \beta\frac{x^2}{2} \tag{37}$$

One can then easily show the stability of motion with the total energy that remains constant with stable motion for $\beta>0$ and no longer stable motion switching between equilibrium states for $\beta<0$; see Fig. 6.

If we now consider damped case with $\delta>0$, such damping term will result with energy dissipation, clearly visible in phase space for either stable of unstable motion trajectories; see Fig. 7.

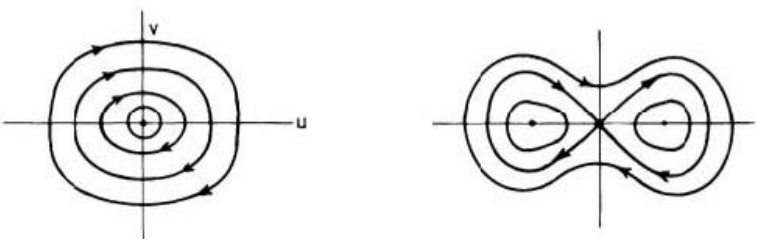

Fig. 6 Phase space representation of Duffing oscillator for non-damped case ($\delta=0$) in free vibrations ($\gamma=0$) with $\beta\geq0$ (left) and $\beta<0$ (right)

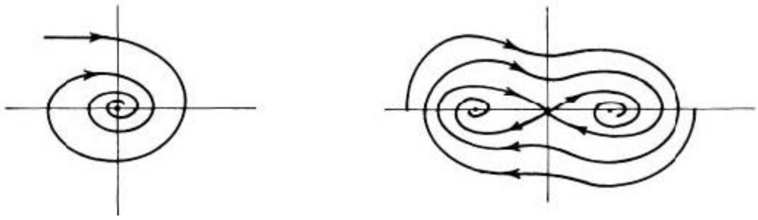

Fig. 7 Phase space representation of Duffing oscillator for damped case (δ>0) in free vibrations (γ=0) with $\beta\geq 0$ (left) and β<0 (right)

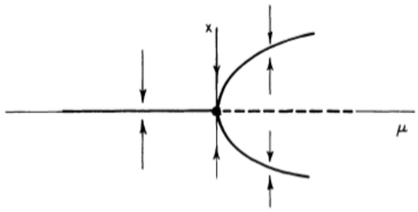

Fig. 8 Pitchfork type bifurcation

For the case of forced vibrations with $\gamma\neq 0$, the phase space representation is no longer by an autonomous system. In order to recover again an autonomous system, we need to increase the dimension of system of equations in phase space representation by introducing a new variable

$$\begin{gathered} \dot{u} = v \\ \dot{v} = -\delta v - \alpha u^3 - \beta u + \gamma \cos(\omega\theta) \\ \dot{\theta} = 1 \end{gathered} \tag{38}$$

where $(u, v, \theta) \in R^2 \times S^1$ (with $S^1 = R/T$ and $T = 2\pi/\omega$).

Intuitively, we can understand well that for a relatively small value of γ, the equilibrium state for the case with δ>0 and $\beta\geq 0$ will be transformed into a periodic orbit round the equilibrium point. The same will apply to two stable equilibrium states for the case with δ>0 and β<0. We note that a small forcing term will be a novel source of energy fluctuation in the system. Hence, the damping is needed here in order to avoid the system motion explosion at the resonance.

One word on bifurcation: We note that passing from one stable equilibrium state to three equilibrium states, with only two of them stable, corresponds to a bifurcation of parameters. The bifurcation in such a differential equation is intimately related to notion of instability and motion trajectories and depends on particular value of parameter β. If for a given β_0 the trajectories of flow in phase space remain stable for a small perturbation of parameter ($\beta_0+\varepsilon$), there is no bifurcation. In the opposite, we conclude that β_0 is the bifurcation parameter value. In Duffing oscillator, the particular case of bifurcation is so-called 'pitchfork' bifurcation (Gukenheimer and Holmes 2013).

5. Stochastic solution to instability problem

5.1 Averaging and asymptotic methods for Duffing oscillator

In this section, we first present couple of computational technics that allow moving beyond qualitative analysis of Duffing oscillator and providing approximate solution for the case of interest of damped forced vibrations. The main hypotheses under which can be carried out concern the systems where applied harmonic loads, damping and nonlinearity are relatively small. Under such hypothesis, one can solve the resonance problem (as dynamics equivalent of instability) by means of methods of averaging and perturbation.

Resonance modes: We will here study the case where we can provide not only qualitative analysis of instability phenomena, but also obtain more quantitative, yet approximate solution (in the absence of analytic solution for forced damped vibrations). This can be done for a special form of instability problem, where we assume that the applied loads, the system damping and nonlinearity are all relatively small (quantified by a small parameter ε). Here, we can provide the solution to instability problem in terms of resonance modes, which is provided by averaging or perturbation methods presented in this section.

With such hypothesis of small loads, damping and nonlinearity, the equation of motion for Duffing oscillator can be written as

$$\ddot{x} + \omega_0^2\, x + \varepsilon\, \delta\, \dot{x} + \varepsilon\, \alpha\, x^3 = \varepsilon\, \gamma\, \cos(\omega t) \tag{39}$$

In order to find different resonance modes of this system, we will assume that solution can be approximated in terms of

$$x(t) = \varepsilon x_1(t) + \varepsilon^2 x_2(t) + \cdots \tag{40}$$

which we inject into the Eq. (39) above. By eliminating further the terms of $O(\varepsilon^2)$, we thus obtain

$$\varepsilon\, \ddot{x}_1 + \varepsilon^2 \ddot{x}_2 + \varepsilon\, \omega_0^2\, x_1 + \varepsilon^2\, \omega_0^2\, x_2 + \varepsilon^2\, \delta\, \dot{x}_1 = \varepsilon\, \gamma\, \cos(\omega t) \tag{41}$$

which gives us, if we separate the terms of $O(\varepsilon)$ and $O(\varepsilon^2)$, the following system of equations

$$\begin{gathered} \ddot{x}_1 + \omega_0^2\, x_1 = \gamma \cos(\omega t) \\ \ddot{x}_2 + \omega_0^2\, x_2 + \delta\, \dot{x}_1 = 0 \end{gathered} \tag{42}$$

We see that x_1 will get into resonance for $\omega \approx \omega_0$, which we call the first resonance mode. We can further have the second resonance mode if x_2 gets into resonance. It can be shown that this happens for $\omega \approx 3\omega_0$ with sup-harmonic resonance or for $\omega \approx \omega_0/3$ for sub-harmonic resonance.

Two methods presented subsequently (averaging and perturbation) consider two time scales in the system, rapid time scale and slow time scale. We discuss them for a particular resonance mode, which is here consider only for the first mode corresponding to $\omega \approx \omega_0$.

Averaging Method: The first solution method for resonance instability problem is referred to as ‘averaging’. As already indicated, here we consider two distinct time scales, slow and fast. These two scales are illustrated in Fig. 9, we carried out computations for chosen numerical values of parameters defined in (39) as: $\omega_0 = \delta = \alpha = 1$ and $\varepsilon = 0.01$. We can see that, given small value of ε, there is a short time corresponding to frequency ω_0 and a long time in system response.

Starting from this observation, we can write the solution in the following format

$$x(t) = u(t) \cos\left(\frac{\omega t}{k}\right) - v(t) \sin\left(\frac{\omega t}{k}\right) \tag{43}$$

In this approximate solution, we assume that $u(t)$ and $v(t)$ vary more slowly than $\cos(\omega t/k)$ or $\sin(\omega t/k)$, which implies that k is such that $\omega \approx k\, \omega_0$ (at the first resonance mode $k=1$). This approximation for $x(t)$ call for following transformation

$$\begin{pmatrix} u \\ v \end{pmatrix} = A \begin{pmatrix} x \\ \dot{x} \end{pmatrix} \tag{44}$$

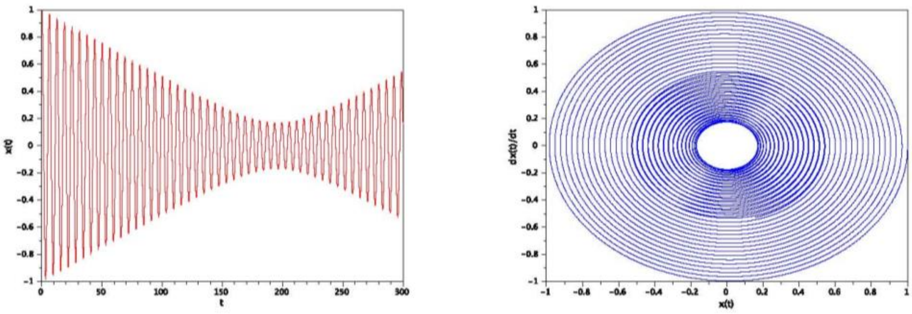

Fig. 9 Computed solution (left) and phase space (right) for Duffing oscillator with numerical values of parameters in (6) chosen as: ω_0=δ=α=1 and ε=0.01

with

$$A=\begin{pmatrix}\cos\frac{\omega t}{k} & -\frac{k}{\omega}\sin\frac{\omega t}{k}\\ -\sin\frac{\omega t}{k} & -\frac{k}{\omega}\cos\frac{\omega t}{k}\end{pmatrix}\ et\ A^{-1}=\begin{pmatrix}\cos\frac{\omega t}{k} & -\sin\frac{\omega t}{k}\\ -\frac{\omega}{k}\sin\frac{\omega t}{k} & -\frac{\omega}{k}\cos\frac{\omega t}{k}\end{pmatrix} \tag{45}$$

By further using the time derivative of the last result leading to

$$\begin{pmatrix}\dot{u}\\ \dot{v}\end{pmatrix}=\dot{A}\begin{pmatrix}x\\ \dot{x}\end{pmatrix}+A\begin{pmatrix}\dot{x}\\ \ddot{x}\end{pmatrix} \tag{46}$$

If we recall that the system is close to the first resonance mode (k=1), and further denote $\omega_0^2-\omega^2=\varepsilon\Omega$, we can easily show that

$$\begin{cases}\dot{u}=\frac{\varepsilon}{\omega}[\Omega(u\cos(\omega t)-v\sin(\omega t))-\gamma\cos(\omega t)-\delta\omega(u\sin(\omega t)+v\cos(\omega t))\\ \qquad +\alpha(u\sin(\omega t)+v\cos(\omega t))^3]\sin\omega\, t\\ \dot{v}=\frac{\varepsilon}{\omega}[\Omega(u\cos(\omega t)-v\sin(\omega t))-\gamma\cos(\omega t)-\delta\omega(u\sin(\omega t)+v\cos(\omega t))\\ \qquad +\alpha(u\sin(\omega t)+v\cos(\omega t))^3]\cos\omega\, t\end{cases} \tag{47}$$

Finally, recalling that $u(t)$ and $v(t)$ vary more slowly than $\cos(\omega t/k)$ or $\sin(\omega t/k)$, we can carry out approximation based upon averaging method. More precisely, we assume that within a single period $T=2\pi/\omega$, values of $u(t), \dot{u}(t), v(t), \dot{v}(t)$ are kept constant. Thus, by integrating over this period T, we obtain an approximation of the last result that can be written as

$$\begin{cases}\dot{u}=\frac{\varepsilon}{2\omega}\left[-\omega\delta u-\Omega v-\frac{3\alpha}{4}(u^2+v^2)v\right]\\ \dot{v}=\frac{\varepsilon}{2\omega}\left[-\omega\delta u+\Omega v-\frac{3\alpha}{4}(u^2+v^2)v-\gamma\right]\end{cases} \tag{48}$$

By solving the system of differential equations above, we get solution for $u(t)$ and $v(t)$. Such solution can also be written in polar coordinates $r=\sqrt{u^2+v^2}$ and $\phi=arc\tan\left(\frac{v}{u}\right)$, leading to

$$\begin{cases}\dot{r}=\frac{\varepsilon}{2\omega}[-\omega\delta r-\gamma\sin\phi]\\ r\dot{\phi}=\frac{\varepsilon}{2\omega}\left[\Omega r+\frac{3\alpha}{4}r^3-\gamma\cos\phi\right]\end{cases} \tag{49}$$

Perturbation Method: We still consider Duffing oscillator motion described by Eq. (35), with parameter ε that has to be small, to quantify the difference of two time scales, fast and slow. However, contrary to averaging method, this difference is now explicitly indicated by choosing

$$\zeta = \omega t, \eta = \varepsilon t \tag{50}$$

where ζ is slow time and η is fast time. Given this explicit representation of time scales, we can further write

$$\begin{aligned} \frac{dx}{dt} &= \frac{\partial x}{\partial \zeta}\frac{d\zeta}{dt} + \frac{\partial x}{\partial \eta}\frac{d\eta}{dt} = \omega \frac{\partial x}{\partial \zeta} + \varepsilon \frac{\partial x}{\partial \eta} \\ \frac{d^2x}{dt^2} &= \omega^2 \frac{\partial^2 x}{\partial \zeta^2} + 2\varepsilon\omega \frac{\partial^2 x}{\partial \zeta \partial \eta} + \varepsilon^2 \frac{\partial^2 x}{\partial \eta^2} \end{aligned} \tag{51}$$

By replacing this result in Eq. (39), we can get

$$\omega^2 \frac{\partial^2 x}{\partial \zeta^2} + 2\varepsilon\omega \frac{\partial^2 x}{\partial \zeta \partial \eta} + \varepsilon^2 \frac{\partial^2 x}{\partial \eta^2} + \omega_0^2 x = \varepsilon\left(\gamma \cos\zeta - \delta\left(\omega \frac{\partial x}{\partial \zeta} + \varepsilon \frac{\partial x}{\partial \eta}\right) - \alpha x^3\right) \tag{52}$$

If we further develop $x(\zeta, \eta)$ and ω in series of ε, such that

$$\begin{cases} x(\zeta,\eta) = x_0(\zeta,\eta) + \varepsilon x_1(\zeta,\eta) + \varepsilon^2 x_2(\zeta,\eta) + \cdots \\ \omega = \omega_0 + \varepsilon k_1 + \varepsilon^2 k_2 + \cdots \end{cases} \tag{53}$$

By combining last two results, and further neglecting the terms of order $O(\varepsilon^2)$, we obtain the following results

$$\begin{cases} \omega_0^2 \dfrac{\partial^2 x_0}{\partial \zeta^2} + \omega_0^2 x_0 = 0 \\ 2\omega_0 k_1 \dfrac{\partial^2 x_0}{\partial \zeta^2} + \omega_0^2 \dfrac{\partial^2 x_1}{\partial \zeta^2} + 2\omega_0 \dfrac{\partial^2 x_0}{\partial \zeta \partial \eta} + \omega_0^2 x_1 = \gamma\cos(\zeta) - \delta\omega_0 \dfrac{\partial x_0}{\partial \zeta} - \alpha x_0^3 \end{cases} \tag{54}$$

from where we can immediately conclude that

$$x_0(\zeta,\eta) = A(\eta)\cos(\zeta) + B(\eta)\sin(\zeta) \tag{55}$$

Hence, the second of Eq. (54) can be written explicitly as

$$\frac{\partial^2 x_1}{\partial \zeta^2} + x_1 = \frac{1}{\omega_0^2}\begin{bmatrix} 2k_1\omega_0(A\,cos(\zeta) + B\,sin(\zeta)) + 2\omega_0 \dfrac{\partial A}{\partial \eta} sin\,\zeta - 2\omega_0 \dfrac{\partial B}{\partial \eta} cos\,\zeta + \gamma\,cos(\zeta) + \\ \delta\omega_0 A\,sin(\zeta) - \delta\omega_0 B\,cos(\zeta) - \alpha(A\,cos(\zeta)\,B\,sin(\zeta))^3 \end{bmatrix} \tag{56}$$

We can write the last result as

$$\frac{\partial^2 x_1}{\partial \zeta^2} + x_1 = \cos(\zeta)\,f_1 + \sin(\zeta)\,f_2 + \cos(3\zeta)\,f_3 + \sin(3\zeta)\,f_4 \tag{57}$$

where f_1, f_2, f_3 and f_4 are functions of k_1, ω_0, η, δ and α. By looking at the last equation, we can see that terms f_1 and f_2 are at the origin of potential explosion of the solution. Thus, following the method of Lindtsted, we will nil these terms knowing that the solution has to remain bounded. Hence by imposing f_1=0 and f_2=0, we obtain

$$\begin{cases} \dfrac{\partial A}{\partial \eta} = \dfrac{1}{2\omega_0}\left(-\omega_0\delta A - 2\omega_0 k_1 B - \dfrac{3\alpha}{4}(A^2 + B^2)B\right) \\ \dfrac{\partial B}{\partial \eta} = \dfrac{1}{2\omega_0}\left(-\omega_0\delta B + 2\omega_0 k_1 A - \dfrac{3\alpha}{4}(A^2 + B^2)A - \gamma\right) \end{cases} \tag{58}$$

The solution of this set of equations gives us the values of A and B. We can easily verify that such a solution provided by perturbation method is of the first order $O(\varepsilon)$ the same as the one already provided by averaging. Namely, by neglecting the terms of the order $O(\varepsilon^2)$ as we have done until now, we will have $\omega=\omega_0+k_1\varepsilon$, and furthermore $\omega_0^2-\omega^2=2\omega_0 k_1 \varepsilon=\varepsilon\Omega$ (by using that $\Omega=2\omega_0 k_1$)

Since, moreover $\frac{dA}{dt}=\frac{\partial A}{\partial\eta}\frac{d\eta}{dt}=\varepsilon\frac{\partial A}{\partial\eta}$ and $\frac{dB}{dt}=\frac{dB}{d\eta}\frac{d\eta}{dt}=\varepsilon\frac{\partial B}{\partial\eta}$, we will finally have

$$\begin{cases}\dot{A}=\frac{\varepsilon}{2\omega_0}\left(-\omega_0\delta A-\Omega B-\frac{3\alpha}{4}(A^2+B^2)B\right)\\ \dot{B}=\frac{\varepsilon}{2\omega_0}\left(-\omega_0\delta B-\Omega A-\frac{3\alpha}{4}(A^2+B^2)B\right)A-\gamma\end{cases} \tag{59}$$

Recall again that by considering the first resonance mode with $\omega\approx\omega_0$, the equations for A and B provided by perturbation become the same as the averaging method provided for u and v.

Both of two methods we presented here for studying the motion of Duffing oscillator, method of averaging and perturbation method, are based upon hypothesis of two distinct time scales (short vs. long). Both methods provide best approximation for the case of small values of applied loads, and system damping and nonlinearity. However, the methods can still be applied to larger values of these parameters, as long as there remain two distinct time scales. However, if system nonlinearity becomes too important, these two approximation methods no longer apply. In fact, the Duffing oscillator in such case would have (much) more complex behavior that tends towards chaotic motion. It is important to note that the notion of chaos is here deterministic (as the consequence of system instability) and not the consequence of introducing any randomness in the system.

5.2 Instability problem with heterogeneous beam with perturbed stochastic equation

In this section we discuss the Euler beam model under joint action of its critical force and a white noise perturbation. Subsequently, we will also consider a more general case where the parameters characterizing the beam are perturbed by a fast stationary ergodic process. That fast evolving process can represent some variation of the material (Moreno-Navarro *et al*. 2021) or the internal variables (Ibrahimbegovic and Mejia-Nava 2021) acting at a different time scale (faster) than the global system. We will see how to model this problem with stochastic differential equation (SDE) and how stochastic averaging can help us to simplify this complex problem.]

Fast perturbation process and stochastic differential equation (SDE): Let us start by considering that the material parameter E (modulus of elasticity) is not constant anymore, but fluctuates quickly over time. More especially, let us consider that E is a function of a fast stationary ergodic stochastic process, denoted by ξ. By 'fast' we mean that the time scale of change (of significant variations) of this process is much shorter than the characteristic time scale of the system vibrations, described by T. We express this difference of time scales by the presence of a small parameter ε, such that we can denote now by $\xi_{/\varepsilon}$ the time rescaled process ξ.

Here we suppose that the modulus of elasticity is subject to fast stationary (and ergodic) fluctuations. Such fluctuations can arise, for example, in the case of MEMS (Micro Electro-Mechanical Systems) where multi-physics interactions have an impact on the material parameters values. For example, a micro mechanical system oscillating in a fast fluctuating electrical field could maybe, under some assumptions, meet our present hypothesis and enter in the scope of this study. Anyway, this assumption gives us a mathematical setting of interest for present case. The exact physical meaning of this fast process can be left open to fit many practical engineering applications.

Under this assumption, we can rewrite the Duffing oscillator equation of motion, driven by a white noise, as follows

$$\ddot{Y}(t) + \left[\frac{\delta}{m}\right]\dot{Y}(t) + \left[\frac{\lambda B}{6mA}\right]Y^3(t) - \left[E\left(\xi_{/\varepsilon}\right)\frac{IC}{mA} + \frac{\lambda}{m}\right]Y(t) = \left(\frac{l}{mA}\right)\widehat{W} \tag{60}$$

Denoting $U_t = \left(\dot{Y}(t), Y(t)\right)^T$, the previous equation can be written as a Stochastic Differential Equation (SDE). Indeed, we have

$$d\begin{pmatrix} Y(t) \\ \dot{Y}(t) \end{pmatrix} = \begin{pmatrix} \dot{Y}(t) \\ -\left(\frac{\delta}{m}\right)\dot{Y}(t) - \left(\frac{\lambda B}{6mA}\right)Y^3(t) + \left(\frac{E(\xi_{\frac{t}{\varepsilon}})IC}{mA} + \frac{\lambda}{m}\right)Y(t) \end{pmatrix} dt + \begin{pmatrix} 0 & 0 \\ 0 & \frac{l}{mA} \end{pmatrix} dW_t \tag{61}$$

which can further be recast is standard format of SDE as

$$dU_t = b\left(U_t, \xi_{/\varepsilon}\right)dt + \sigma dW_t \tag{62}$$

with model parameters b and σ can be defined by matching expressions in (61) and (62).

We are now interested by the behavior of this system when the difference of time scales between the evolution of the global system and the much faster evolution of the fast perturbation process becomes larger and larger. This more and more important separation of time scales is mathematically expressed by a parameter ε that gets closer and closer to 0.

Many questions arise from such a situation, the chief among them if there is any convergence that can be observed when $\varepsilon \to 0$, and if there is, under which assumptions. Moreover, we can also ask if the case of a noise depending on the state of the system (multiplicatively, such that $\sigma(U_t)$) leads to result convergence, and what are differences and similarities between various cases.

All this kind of questions enter in the field of mathematical limits theorems for stochastic processes. In the next few pages we try to give an overview of the subject of interest, of questions that can already be answered and of questions that remain open for the moment.

In this section, we will briefly discuss the general mathematical setting and problems of convergence. First, we will rewrite our equation of interest in the notation that can be found, most of the time, in the literature. Then we will divide the problem in three sub-cases of increasing difficulties.

Let us first consider here a standard SDE written in the differential form

$$\begin{cases} dX(t) = b\left(X(t)\right)dt + \sigma\left(X(t)\right)dW(t) \\ X_0 = x_0 \end{cases} \tag{63}$$

where: σ is $n \times d$–matrix, b n–dimensional vector, $W(t)$ is d–dimensional Brownian motion (Wiener process).

Theorem: Suppose that coefficient sig and b are locally Lipschitz, that is for any $A>0$, there exists a constant $K>0$, depending only on A and T, such that, for all $|x| \vee |y| \le A$ and $0 \le t \le T$

$$\|b(x) - b(y)\| + \|\sigma(x) - \sigma(y)\| < K\|x - y\| \tag{64}$$

where $\|b\| = \left\{\sum b_i^2\right\}^{\frac{1}{2}}$ and $\|\sigma\|^2 = T(\sigma\sigma^T)$

Then for any given initial point $X(0)$ the SDE (63) has a unique strong solution on $[0, T]$. Moreover

$$\mathbb{E}\left(\sup_{0\leq t\leq T}\|X(t)\|^2\right) \leq C(1+\mathbb{E}\|X(0)\|^2) \tag{65}$$

where C depends only on T and K.

We are interested in stochastic averaging approach when this initial SDE is perturbed in its coefficients by a fast stationary ergodic stochastic process, denoted by ξ. By 'fast' we mean that the time scale of change (of significant variations) of this process is much shorter than the time scale of the system described by the stochastic process X. That is why we speak about fast perturbation process. We express this difference of time scales by the presence of a really small parameter ε such that we consider now $\xi_{t/\varepsilon}$ (the time rescaled process ξ). We can then rewrite

$$\begin{cases} dX_t^\varepsilon = b\left(X_t^\varepsilon, \xi_{t/\varepsilon}\right)dt + \sigma\left(X_t^\varepsilon, \xi_{t/\varepsilon}\right)dW_t \\ \quad X_0^\varepsilon = x_0 \end{cases} \tag{66}$$

Of course, for different reasons, it is of great interest to be able to characterize the behavior of the process X^ε when ε goes to 0. For example, the limiting behavior will be a good approximation when ε is close to 0 to the effective behavior of the system. It could become really interesting for simulations, analytic studies or any other approach that prefer a simpler system to consider.

If proofs of convergence already exist and can be found in many classical textbook (see, [1] or [2]), most of these results rely at least on two assumptions on the coefficients b and σ: i) global Lipschitz and their linear growth in the first variable; for example, we ask for b (and the same for σ) that

$$\begin{cases} \exists L \;\text{ such that }\; |b(x,y)-b(z,y)| \leq L|x-z| \;\text{ uniformly in } y \\ \exists C \;\text{ such that }\; |b(x,y)| \leq C(|x|+1) \;\text{ uniformly in } y \end{cases} \tag{67}$$

Note that these conditions are not really two distinct conditions, since the first one leads in (almost) straightforward way to the second. We make the distinction clear here in order to make appear what they are used for in the proofs.

Roughly speaking, we can see that these conditions are the necessary ones to ensure the compactness of the family $(X^\varepsilon)_{\varepsilon>0}$. Indeed, we can state that

- the linear growth condition will ensure the non-explosiveness (in terms of mean and variability) in finite time of the solution and then constitute roughly the first required part to prove the tightness,
- the Lipschitz condition will ensure the solution increase remains bounded, which constitutes the second requirement to prove the compactness.

If the compactness can be proved, then the remaining task to show the convergence result is a little bit easier and will use absolutely fundamental ergodic principle to characterize any converging subsequence.

At this point, it should be noticed that the few previous lines are just supposed to give a very rough idea of what existing results use in their proofs, why assumptions are important for and can be lose if we do not consider this assumption true anymore. Obviously, the results are very difficult to obtain and their proofs sometimes rely on technical points that goes far beyond the description given in this document. We refer to [2] and [1] for details about these proofs.

Now, beyond these existing results on the subject, we are interested here to know when it is possible to relax these hypotheses and how to do this. For example, what can be said if b and σ does not satisfy global Lipschitz condition, but only its local version.

While the case without the stochastic integral term has been more widely studied, results are less abundant for the case with the stochastic integral term. We can divide the difficulty and the result that can be obtained in 3 parts, considering the 3 following kind of systems, that go in the order of increasing the problem difficulty:

i) constant σ case

$$\begin{cases} dX_t^\varepsilon = b\left(X_t^\varepsilon, \xi_{\frac{t}{\varepsilon}}\right)dt + \sigma dW_t \\ X_0^\varepsilon = x_0 \end{cases} \tag{68}$$

ii) non-constant, but non-perturbed σ case

$$\begin{cases} dX_t^\varepsilon = b\left(X_t^\varepsilon, \xi_{\frac{t}{\varepsilon}}\right)dt + \sigma(dX_t^\varepsilon)dW_t \\ X_0^\varepsilon = x_0 \end{cases} \tag{69}$$

iii) non-constant and perturbed σ case

$$\begin{cases} dX_t^\varepsilon = b\left(X_t^\varepsilon, \xi_{\frac{t}{\varepsilon}}\right)dt + \sigma\left(dX_t^\varepsilon, \xi_{\frac{t}{\varepsilon}}\right)dW_t \\ X_0^\varepsilon = x_0 \end{cases} \tag{70}$$

For the remaining part of the paper, denoting $\rho(dy)$ as the law of the stationary ergodic process ξ, let us also define $\overline{b}$ and $\bar{\sigma}$ such that

$$\bar{b}(x) = \int b(x, y)\rho(dy) \tag{71}$$

and

$$\bar{\sigma}(x)\bar{\sigma}^*(x) = \int \sigma(x, y)\sigma^*(x, y)\rho(dy). \tag{72}$$

Note that here and in the foregoing, we denote the dependence of any different stochastic process on the probability space as implicit. Thus, with the full probability space denoted by Ω and a particular realization by ω, we further write X_t^ε instead of $X_t^\varepsilon(\omega)$ or $\xi_{./\varepsilon}$ instead of $\xi_{./\varepsilon}(\omega)$.

i) constant σ case: We first consider here the solution of SDE with constant σ

$$\begin{cases} dX_t^\varepsilon = b\left(X_t^\varepsilon, \xi_{\frac{t}{\varepsilon}}\right)dt + \sigma dW_t \\ X_0^\varepsilon = x_0 \end{cases} \tag{73}$$

where ξ denotes the stationary ergodic process as described previously and σ is a constant that satisfies the following hypotheses:

($h1$) for any compact set K, there exists L_K such that $|b(x, y) - b(z, y)| \leq L_K|x - z|$ uniformly in y provided $x \in K$ and $z \in K$ (local Lipschitz condition),

It is worth noticing that assumption (h1) implies that function $\bar{b}$ is also locally Lipschitz with the same constant L_K for a compact set K, and moreover $\bar{b}$satisfies the same linear growth relation (67) as b with the same constant C.

$$\begin{cases} d\bar{X}_t = \bar{b}(\bar{X}_t)dt + \sigma dW_t \\ \bar{X}_0 = x_0 \end{cases} \tag{74}$$

Proposition 4.1. Under hypotheses ($h1$) and ($h2$), it can be shown that for any T>0 we have almost surely

$$\lim_{\varepsilon\to 0}\sup_{0\le t\le T}|X_t^\varepsilon - \bar{X}_t| = 0 \tag{75}$$

Proof. Let us consider a fixed value of $T>0$. By hypotheses ($h2$), there exist a subset Ω' of probability 1 of the probability space Ω such that for any realization $\omega\in\Omega'$ there exists finite values m and M such that $\sup_{0\le t\le T}|\bar{X}_t| \le m < M$. In the following, we consider a realization $\omega\in\Omega'$.

Define then $\tau_M^\varepsilon = inf\{t \ge 0: |X_t^\varepsilon \ge M|\}$. Then we have for any $t \in [0; T\wedge\tau_M^\varepsilon]$

$$\begin{aligned}
\left|X_t^\varepsilon - \bar{X}_t\right| &= \left|\int_0^t b\left(X_s^\varepsilon,\xi_{s/\varepsilon}\right) - \bar{b}\left(\bar{X}_s\right)ds\right| \\
&= \left|\int_0^t b\left(X_s^\varepsilon,\xi_{s/\varepsilon}\right) - b\left(\bar{X}_s,\xi_{s/\varepsilon}\right)ds + \int_0^t b\left(\bar{X}_s,\xi_{s/\varepsilon}\right) - \bar{b}\left(\bar{X}_s\right)ds\right| \\
&\le L_M\int_0^t\left|X_s^\varepsilon - \bar{X}_s\right|ds + \left|\int_0^t b\left(\bar{X}_s,\xi_{s/\varepsilon}\right) - \bar{b}\left(\bar{X}_s\right)ds\right|
\end{aligned} \tag{76}$$

We denote $R(T,\varepsilon) = \sup_{0\le t\le T}\left|\int_0^t b\left(\bar{X}_s,\xi_{\frac{s}{\varepsilon}}\right) - \bar{b}(\bar{X}_s)ds\right|$ and note that by hypothesis ($h2$) and the standard Birkhoff ergodic theorem, for any fixed $T>0$, $R(T, \varepsilon)\to 0$ almost surely, as $\varepsilon\to 0$. We denote by Ω'' the subset of probability 1 of the probability space Ω on which the Birkhoff ergodic theorem is verified. In the following, we consider a realization $\omega\in\Omega'\cap\Omega''$

By Eq. (24) and Gronwall lemma we have for any $t \in [0; T\wedge\tau_M^\varepsilon]$

$$\sup_{0\le t\le T\wedge\tau_M^\varepsilon}|X_t^\varepsilon - \bar{X}_t| \le \sup_{0\le t\le T\wedge\tau_M^\varepsilon} R(T,\varepsilon)\,exp(L_M t) \le R(t,\varepsilon)\,exp(L_M t) \underset{\varepsilon\to 0}{\to} 0 \tag{77}$$

By (77), it obviously comes that there exists ε' such that for all $\varepsilon<\varepsilon'$ we have $\sup_{0\le t\le T\wedge\tau_M^\varepsilon}|X_t^\varepsilon| < M$ and then, for all $\varepsilon<\varepsilon'$, we have $\tau^\varepsilon > T$. We can then conclude that

$$\lim_{\varepsilon\to 0}\sup_{0\le t\le T\wedge\tau_M^\varepsilon}|X_t^\varepsilon - \bar{X}_t| = \lim_{\varepsilon\to 0}\sup_{0\le t\le T}|X_t^\varepsilon - \bar{X}_t| = 0 \tag{78}$$

This being true for any realization $\omega\in\Omega'\cap\Omega''$, the result is well proven almost surely (because $\Omega'\cap\Omega''$ is of probability 1).

Remark 4.1. The main difference between the assumption stated here and the one previously discussed is the following. In the condition stated here, nothing is assumed on the global Lipschitz of the system. So, as this hypothesis is relaxed, the counterpart is that we need to assume something on the averaged solution in order to prove the result.

ii) non-constant, but non-perturbed σ case : We consider now the solution of

$$\begin{cases} dX_t^\varepsilon = b\left(X_t^\varepsilon,\xi_{\frac{t}{\varepsilon}}\right)dt + \sigma(X_t^\varepsilon)dW_t \\ X_0^\varepsilon = x_0 \end{cases} \tag{79}$$

with ξ the stationary ergodic process as in the introduction of this document, σ a function only of the state of the solution (but not impacted by the fast perturbation process ξ) and such that the following hypotheses are satisfied:

($h1$) for any compact set K, there exists L_K such that $|b(x,y)-b(z,y)| \leq L_K|x-z||\sigma(x)-\sigma(z)| \leq L_K|x-z|$ (uniformly in y) and provided $x \in K$ and $z \in K$ (local Lipschitz for b and σ), ($h2$) the solution of

$$\begin{cases} d\bar{X}_t = \bar{b}(\bar{X}_t)dt + \sigma(\bar{X}_t)dW_t \\ \bar{X}_0 = x_0 \end{cases} \tag{80}$$

almost surely exist, is continuous and is defined over $[0;+\infty)$ almost sure non-explosiveness in finite time of the averaged solution.

For this case, simulations seem to show that almost sure convergence still holds. This belief is reasonable in the sense that the fast perturbation process ξ does not impact the coefficient σ. Then, $\sigma(X^\varepsilon)$ still vary much more slowly than W, no matter ε, making the almost sure convergence possible. The results still need to be proved. Maybe these hypotheses are not suffcient to prove the result. The work still needs to be done here.

iii) non-constant, but perturbed σ case: We consider now the solution of

$$\begin{cases} dX_t^\varepsilon = b\left(X_t^\varepsilon, \xi_{\frac{t}{\varepsilon}}\right)dt + \sigma\left(X_t^\varepsilon, \xi_{\frac{t}{\varepsilon}}\right)dW_t \\ X_0^\varepsilon = x_0 \end{cases} \tag{81}$$

with ξ the stationary ergodic process as in the introduction of this document, σ a function of the state of the solution and of the fast perturbation process ξ and such that the following hypotheses are satisfied:

($h1$) for any compact set K, there exists L_K such that $|b(x,y)-b(z,y)| \leq L_K|x-z|$ and $|\sigma(x,y)-\sigma(z,y)| \leq L_K|x-z|$ uniformly in y provided $x \in K$ and $z \in K$ (local Lipschitz for b and σ), ($h2$) the solution of

$$\begin{cases} d\bar{X}_t = \bar{b}(\bar{X}_t)dt + \bar{\sigma}(\bar{X}_t)dW_t \\ \bar{X}_0 = x_0 \end{cases} \tag{82}$$

almost surely exist, is continuous and is defined over $[0;+\infty)$ almost sure non-explosiveness in finite time of the averaged solution.

For this case, it is pretty clear that almost sure convergence does not hold. The reason why we lose the almost sure convergence is due to the fact the now σ is also function of the fast perturbation process ξ. Then, when ε goes to 0, the fluctuations of $\sigma\left(X_t^\varepsilon, \xi_{\frac{t}{\varepsilon}}\right)$ can be as fast as the one of W making that the averaging process won't take place point-wise but also in law.

Again, results of this kind have already been proven but not under these kinds of assumptions. Assumptions and proof still need to be further worked out.

5.3 Instability problem solution with stochastic equation for Duffing oscillator

In this section, we are interested in finding the solution to nonlinear response of the Duffing oscillator under loading that is represented by normalized Gaussian white noise. In particular, we are interested in finding the stationary law for Duffing oscillator. This will be done both by clarifying the conditions for solution existence of stochastic differential equation (SDE), and by numerical computations for Duffing oscillator stationary law in terms of Fokker-Planck equation.

The problem we are interested in of nonlinear random vibrations for Duffing oscillator is but one of the problems that can be described by SDE coming from various applications. In fact, such problems are found in modeling the wind loads, seismic loads or any other stochastic load applied to vibrating structure. The probability studies of such stochastic loads also allow estimating the structure reliability with respect to risk of rupture or fatigue failure.

Here, we will focus upon SDE that can be used to describe oscillations of mechanical system, written for a scalar field

$$\begin{cases} \ddot{x}(t) + f\big(\dot{x}(t), x(t)\big) = \eta \dot{W}(t) \\ \dot{x}(0) = \dot{x}_0 \text{ p.s.} \\ x(0) = x_0 \text{ p.s.} \end{cases} \tag{83}$$

where *W* is Wiener normalized process with values in *R*, *W*' is its derivative in the sense of distribution (i.e., the normalized Gaussian white noise with values in *R*; see (Arnold 1974), ch. 3 for more details). Finally, $(\dot{x}_0; x_0)$ is random variable in R^2 independent of process *W*. If we now place the development in phase space, denoting $X(t) = (x(t); \dot{x}(t))^t$, we can rewrite Eq. (83) as a classical stochastic differential equation

$$\begin{cases} dX(t) = b\big(X(t)\big)dt + \sigma\big(X(t)\big)dW(t) \\ X(0) = X_0 \text{ p.s.} \end{cases} \tag{84}$$

where we have

$$b\big(X(t)\big) = \begin{pmatrix} \dot{x}(t) \\ -f\big(\dot{x}(t), x(t)\big) \end{pmatrix} \; ; \; \sigma\big(X(t)\big) = \begin{pmatrix} 0 \\ \eta \end{pmatrix} \tag{85}$$

We are interested in SDE of type (84) or its equivalent type (86). We will seek to establish existence of stationary probability law. In the case of existence of such law, we further seek to compute it, or at least to approximate it. We can also seek to define the necessary conditions on equation (namely on damping term) that can avoid the explosion of system motion. We note here that stochastic load is Gaussian white noise. However, it is only a partial loss of generality, given that the case with colored Gaussian process, the method referred to whiting (via Markov process, indicated in (Ethier and Kurz 2009) will allow us to again reduce the problem to white noise loading.

Solution existence: in this section, we will introduce the existence results in a somewhat more general framework that the one set by SDE in Eq. (84). We also introduce the definition of the generator of a SDE. Let us consider solution of a SDE

$$X(t) = X(t_0) + \int_{t_0}^{t} b\big(X(s)\big)ds + \sum_{r=1}^{k} \int_{t_0}^{t} \sigma_r\big(X(s)\big)dW_r(s) \tag{86}$$

where $X(t)$ \in R^n, $X(t_0)$ is a random variable with values in R^n, and where W_r are independent normalized Wiener processes with values in R. We have the following theorem (see [3], ch. 3)

Theorem 2.1 If $b(s,x)$, $\sigma_1(s,x)$, $\sigma_2(s,x)$, …, $\sigma_k(s,x)$ are continuous functions on $[t_0, T]$ x $R^n \rightarrow R^n$, such that there exists a constant verifying

$$|b(x) - b(y)| + \sum_{r=1}^{k} |\sigma_r(x) - \sigma_r(y)| \leq C|x - y| \tag{87}$$

$$|b(x)| + \sum_{r=1}^{k} |\sigma_r(x)| \leq C(1 + |x|) \tag{88}$$

then for any random variable $X(t_0)$ independent of stochastic process ($W_r(t)$; t>0) there exists a solution of Eq. (84), which is a stochastic process almost surely continuous and unique.

Let us now consider process $X(t)$ that verifies Eq. (86), as well as a function $V(t; x)$ $((t; x)\in[t_0; T] \text{ x } R_n)$, which allows partial derivative until order 2 in x and order 1 in t. The differential formula of Ito gives us (denoting $a = \sigma\sigma^T$).

$$dV\big(X(t)\big) = \left[\sum_{i=1}^{n} b_i\big(X(t)\big)\frac{\partial V\big(X(t)\big)}{\partial x_i} + \frac{1}{2}\sum_{i=1}^{n}\sum_{j=1}^{n} a_{ij}\big(t, X(t)\big)\frac{\partial^2 V\big(X(t)\big)}{\partial x_i \partial x_j}\right]dt + \sum_{i=1}^{n}\sum_{r=1}^{k}\sigma_{r_i}\big(X(t)\big)\frac{\partial V\big(X(t)\big)}{\partial x_i}dW_r(t) \tag{89}$$

or yet in integral form

$$V\big(X(t)\big) = V\big(X(t_0)\big) + \int_{t_0}^{t} LV\big(X(u)\big)du + \sum_{i=1}^{n}\sum_{r=1}^{k}\int_{t_0}^{t}\sigma_{r_i}\big(X(u)\big)\frac{\partial V\big(X(u)\big)}{\partial x_i}dW_r(u) \tag{90}$$

where L is the generator of the Markov process $X(t)$, which defined so that for any function $V(X(t))$ $((t; x)\in[t_0; T]x\mathrm{R}_n)$ we have

$$LV\big(X(t)\big) = \sum_{i=1}^{n} b_i\big(X(t)\big)\frac{\partial V\big(X(t)\big)}{\partial x_i} + \frac{1}{2}\sum_{i=1}^{n}\sum_{j=1}^{n} a_{ij}\big(X(t)\big)\frac{\partial^2 V\big(X(t)\big)}{\partial x_i \partial x_j} \tag{91}$$

5.4 Duffing oscillator

Duffing equation: we will further specialize our development for the case where $f(\dot{x}(t); x(t)) = \delta\dot{x}(t) + \alpha x^3(t) + \beta x(t)$, where δ>0, α>0. We will thus have

$$\begin{cases} \ddot{x}(t) + \delta\dot{x}(t) + \alpha x(t)^3 + \beta x(t) = \eta\dot{W}(t) \quad , \quad \eta > 0 \\ \big(\dot{x}(0), x(0)\big) = (\dot{x}_0, x_0) \text{ p.s.} \end{cases} \tag{92}$$

Here, the damping term being always positive, the energy of the system that is not loaded by any external loads will diminish until finally becoming equal to zero. For a=d=b=1 and $(\dot{x}_0, x_0) = (0,1)$, we have represented deterministic behavior of the oscillator (with no stochastic loads), as well as one possible trajectory of the same oscillator loaded by white noise. The computations are performed by using the Euler time integration scheme when applying deterministic loads and by using the Euler-Maruyama scheme when applying a white noise loading.

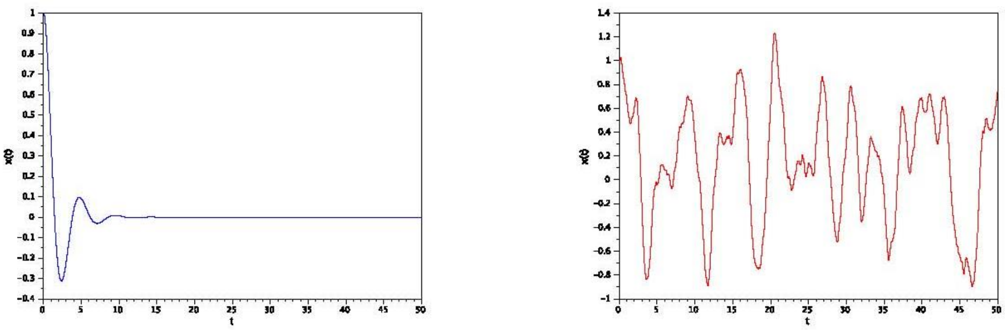

Fig. 10 Response of Duffing oscillator under deterministic load (left) and white noise (right)

For Duffing oscillator, by denoting $y(t) = \dot{x}(t)$, we have $x(t)$, $y(t)$ as bi-dimensional Markov process verifying the following SDE

$$d\begin{pmatrix} x(t) \\ y(t) \end{pmatrix} = \begin{pmatrix} y(t) \\ -\big(\delta y(t) + \alpha x(t)^3 + \beta x(t)\big) \end{pmatrix} dt + \begin{pmatrix} 0 \\ \eta \end{pmatrix} dW(t) \quad , \quad \eta > 0 \tag{93}$$

for which the generator takes the form

$$L = y\frac{\partial}{\partial x} - (\delta y + \alpha x^3 + \beta x)\frac{\partial}{\partial y} + \frac{\eta^2}{2}\frac{\partial^2}{\partial y^2} \tag{94}$$

The stationary law of the above diffusion process $X(t)$, if it exists, is given by

$$L^* p = 0 \tag{95}$$

where L^* is the adjoint operator of L.

Existence of stationary law: The first important question concerning Duffing oscillator concerns the existence of a stationary law for bi-dimensional process $X(t) = (x(t), \dot{x}(t))$. In order to prove the existence of a stationary law, we will exploit the theorem (Khasminskii 2012), which can be written for the general case as:

Theorem 5.1: If coefficients b and σ in Eq. (86) verify conditions in (87) and (88) in an open ball of radius $R>0$, if there exists a real-valued function $V \in C^2(R^n)$, that satisfies

$$V(x) \geq 0, \tag{96}$$

and

$$\sup_{|x|>R} LV(x) = -A_R \rightarrow -\infty \ \text{ when } \ R \rightarrow \infty \tag{97}$$

where L is the operator defined in (94), and if $X(t)$ is regular, we then conclude the solution existence for (95) for which the law is stationary.

We will start by verifying that coefficients b and σ verify the conditions in (87) and (88), and if the process is regular. As suggested by an example proposed by Nevelson, we can take as function $V(x,y)$ to verify conditions (96) and (97)

$$V(x,y) = \frac{y}{2} + (\delta x - \gamma\, arc\tan(x))y + \alpha\frac{x^4}{4} + \beta\frac{x^2}{2} + \delta\int_0^x (\delta u - \gamma\, arc\tan(u))du + k \tag{98}$$

with γ and k well chosen (positive).

$$V(x,y) = \frac{(y+\delta x-\gamma\, arc\tan(x))^2}{2} - \frac{(\gamma\, arc\tan(x))^2}{2} + \alpha\frac{x^4}{4} + \beta\frac{x^2}{2} + \delta\gamma\int_0^x \frac{u}{1+u^2}du + k \tag{99}$$

First, we can evidently show that $\frac{(y+\delta x-\gamma\, arc\tan(x))^2}{2} \geq 0$ and $-\frac{(\gamma\, arc\tan(x))^2}{2} \geq -\frac{(\gamma\pi)^2}{8}$. Moreover, given that we choose $\alpha>0$, we can confirm that there exist a constant k' such that $\alpha\frac{x^4}{4} + \beta\frac{x^2}{2} > \dot{k}$. If we choose a positive value for γ, we will also have $\delta\gamma\int_0^x \frac{u}{(1+u^2)}du \geq 0$. Finally, we will have $V(x,y) \geq -\frac{(\gamma\pi)^2}{8} + \dot{k} + k$.

We can also easily verify that

$$\begin{aligned} LV(x,y) &= y\frac{\partial}{\partial x}V(x,y) - \left(\delta y + \alpha x^3 + \beta x\right)\frac{\partial}{\partial y}V(x,y) + \frac{\eta^2}{2}\frac{\partial^2}{\partial y^2}V(x,y) \\ &= -\frac{\gamma}{1+x^2}y^2 - \left(\alpha x^3 + \beta x\right)\left(\delta x - \gamma \arctan(x)\right) + \frac{\eta^2}{2} \end{aligned} \tag{100}$$

In order to verify (96), it is enough to show, by choosing x=r cosθ and y=r sinθ, that

$$\lim_{r\to\infty} \sup_{z\in[0;1]} -\frac{\gamma}{1+r^2z^2}r^2(1-z^2)-(\alpha r^3z^3+\beta rz)(\delta rz-\gamma\, arc\tan(rz))+\frac{\eta^2}{2}=-\infty \tag{101}$$

Hence, it is clear (recalling that α>0, δ>0 and γ>0) that $\vee z$ €[0,1] fixed, we will have

$$\lim_{r\to\infty} -\frac{\gamma}{1+r^2z^2}r^2(1-z^2)-(\alpha r^3z^3+\beta rz)(\delta rz-\gamma\, arc\tan(rz))+\frac{\eta^2}{2}=-\infty \tag{102}$$

which allows to conclude the proof. Thus, by choosing γ and k positive such that $k \geq -\frac{(\gamma\pi)^2}{8}+\dot{k}$, function $V(x,y)$ will verify (96) and (97). Theorem 5.1 allows us to confirm existence of stationary law, of the process $X(t)$. The density of the distribution is given as solution of Eq. (95) as we can see in the next paragraph.

Computation of stationary law: Here we will further be interested in computing the stationary law for Duffing oscillator system. To that end, we will exploit the Fokker-Planck equation. Let us consider the SDE in (93). If coefficients b and σ verify conditions (98) and (88), we know that the SDE will allow a unique solution for all random variables $X(t_0)$. We know that the transition probability $P(s, y; t, dx)=P(X(t)\in dx|X(s)=y)$ (or conditional probability that $X(t)$ belongs to dx given that $X(s)=y$, with $0\leq s\leq t$) is a solution of the Fokker-Planck partial differential equation. By supposing that $P(s, y; t, dx)$ is sufficiently regular to allow defining the probability density function $P(s, y; t, dx)=p(s, y; t, x)dx$, we have

$$\frac{\partial p(s,y,t,x)}{\partial t}+\sum_{j=1}^{n}\frac{\partial\left(b_j(x)p(s,y,t,x)\right)}{\partial x_j}-\frac{1}{2}\sum_{i=1}^{n}\sum_{j=1}^{n}\frac{\partial^2\left(a_{ij}(x)p(s,y,t,x)\right)}{\partial x_i\partial x_j}=0 \tag{103}$$

We note now the stationary law as $P_s(dx)=p_s(x)dx$. By definition, this stationary law verifies ($0\leq s\leq t$), the following equation

$$p_s(x)=\int_{-\infty}^{+\infty}p(s,y,t,x)p_s(y)dy \tag{104}$$

By multiplying (103) by $p_s(y)$ and integrating, we obtain the reduced Fokker-Planck equation

$$\sum_{j=1}^{n}\frac{\partial\left(b_j(x)p_s(x)\right)}{\partial x_j}-\frac{1}{2}\sum_{i=1}^{n}\sum_{j=1}^{n}\frac{\partial^2\left(a_{ij}(x)p_s(x)\right)}{\partial x_i\partial x_j}=0 \tag{105}$$

The solution of this PDE gives the stationary law as a stationary solution $X(t)$ of SDE in (93), if such stationary solution exists.

For Duffing equation, we have already shown that Eq. (103) admits a solution for stationary law. The corresponding reduced Fokker-Planck can be written as

$$y\frac{\partial p_s(x,y)}{\partial x}+\frac{\partial\left(-\left(\delta y+\alpha x^3+\beta x\right)p_s(x,y)\right)}{\partial y}-\frac{\eta^2}{2}\frac{\partial^2 p_s(x,y)}{\partial y^2}=0 \tag{106}$$

This equation admit an analytic solution (see [2] for more details on solution method) leading to: $p_s(x,y)=Ce^{\left[-\delta\left(y^2+\frac{\alpha x^4}{2}+\beta x^2\right)\right]}$, where C is a normalization constant. If we are only interested in stationary law, that we denote as $p_s(x)$ by abuse of notation, we obtain

$$p_s(x)=\int_{-\infty}^{+\infty}p_s(x,y)dy=\dot{C}e^{-\delta\left[\left(\frac{\alpha x^4}{2}+\beta x^2\right)\right]} \tag{107}$$

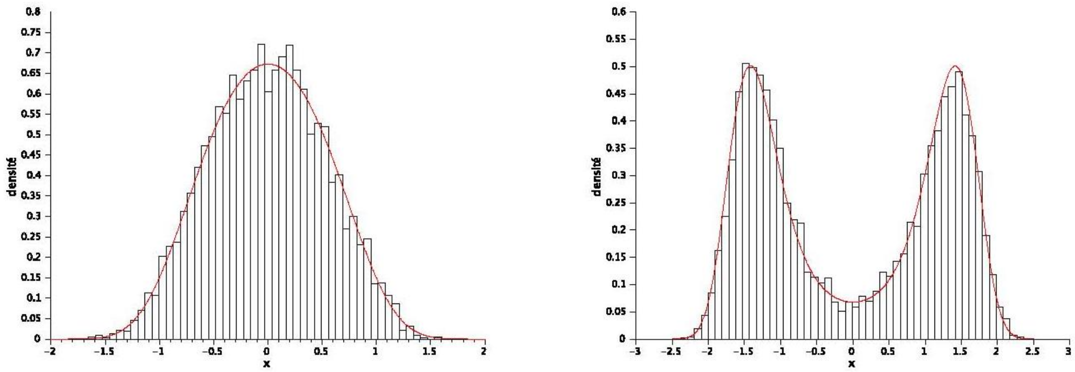

Fig. 11 Stationary solution for system in (14), with exact (red line) and numerical (histogram) with parameters values `δ=α=β=η=1 (left) vs. δ=α=η=1 and β=−2 (right)

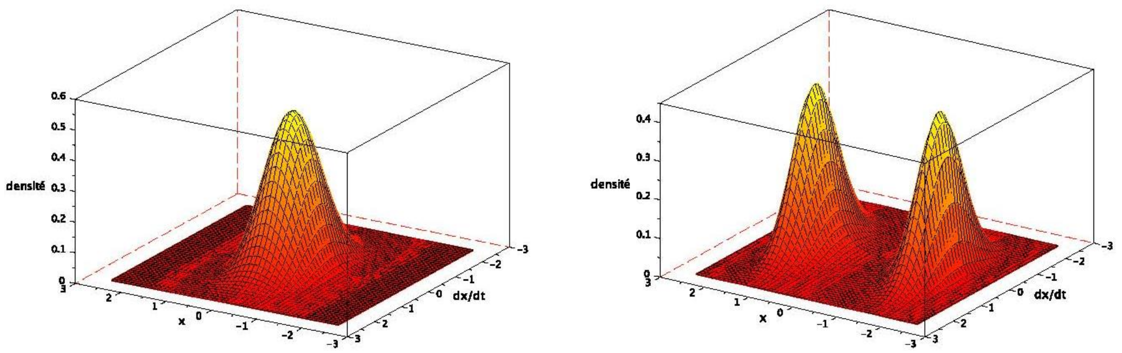

Fig. 12 Exact solution for stationary law for system in (14) for parameters `δ=α=β=η=1 (left) and for parameters δ=α=η=1 and β=−2 (right)

In Fig. 11 we have represented the stationary solution of position x for the considered system, obtained by numerical simulation using the Monte-Carlo method, as well as exact solution obtained for different values of parameters. In Fig. 12, we have represented the exact stationary law of the couple position/velocity (x and $y = \dot{x}$) for different values of parameters.

5. Conclusions

In this paper we have revisited the classical problem of instability of the Euler beam under conservative loading, presenting several possible approaches that are validated against known analytic solution, but that can also be applied to solve instability problems of structures that are (much) more complex from Euler's cantilever.

In particular, we have first demonstrated numerical approach based upon the discrete approximation constructed by using the corresponding weak form of the problem and the finite element method. The key ingredient of such an approach is the use of the von Karman virtual strain (along with linearized real strain and linear elastic constitutive equation) that is proved capable of converging to the exact solution to this classical problem by using more refined finite element mesh with increased number of elements. Moreover, we have shown that such an approach can easily generalized to heterogeneous beam material, and still deliver the corresponding solution without need to change any step in the numerical solution procedure. This is shown on the example of heterogeneous elastic material for the Euler beam, with (fast) period variation that can finally converge to the instability problem solution for homogenized beam. Thus, we showed that for larger defects of coarse finite element mesh the instability problem solution is not the same for homogeneous versus heterogeneous beam. Thus, homogenization problem and linear instability problem do not always commute.

We have also shown that the linearized buckling solution can be recovered as the corresponding bifurcation point when using geometrically exact beam model. This comes as no surprise, since we showed that the consistent linearization of geometrically exact beam model, along with constraints on zero axial deformation (inextensible beam) and zero shear deformation, allow us to recover the same governing equation for linearized instability.

However, we can also keep higher order terms and prepare the governing equations of reduced model that allows to replace cantilever beam instability problem by the Duffing oscillator. The latter is constructed by combining the discrete approximation and dynamics framework for such instability problem in order to provide a 0D model where the beam vibration is reduced to a single material point with corresponding generalized nonlinear stiffness, lumped mass and damping coefficients. We further consider that such a system is excited first by fast oscillating harmonic force, which allowed us to illustrate the corresponding approximate solutions for instability problems in terms of Hamiltonian when two time scales are present in the problem.

Finally, we have presented the stochastic solution to the Euler beam instability problem, by making us of reduced model constructed in terms of the Duffing oscillator. We have used the same kind procedure to solve this instability problem in the stochastic framework brought about the white noise stochastic process used as excitation replacing fast harmonic loads. We showed that we are able to construct the corresponding probability distribution by solving Fokker-Planck equations for instability solution. This is shown both for homogeneous beam material and for beam material heterogeneities described in terms of fast oscillating stochastic process, which is typical of time evolution of internal variables describing plasticity and damage. The additional computational cost of stochastic framework is to a large extent compensated by overall estimate of instability load for heterogeneous materials.

Acknowledgements

This work was supported by funding from ANR (project MS3C), MEAE (project CESPA) and IUF (project MS1479). All this support is gratefully acknowledged.

References

Arnold, L. (1974), *Stochastic Differential Equations: Theory and Applications*, John Wiley.

Cai, G.Q. and Lin, Y.K. (1988), “On exact stationary solutions of equivalent non-linear stochastic systems”, *Int. J. Nonlin. Mech*., **23**(4), 315-325.

Clough, R.W. and Penzien, J. (2006), *Dynamics of Structures*, MsGraw-Hill.

Culver, D., McHugh, K.A. and Dowell, E.H. (2019), “An assessment and extension of geometrically nonlinear beam theories”, *Mech. Syst. Signal Pr.*, **134**, 106340. https://doi.org/10.1016/j.ymssp.2019.106340.

Dujc, J., Brank, B. and Ibrahimbegovic, A. (2010), “Multi-scale computational model for failure analysis of metal frames that includes softening and local buckling”, *Comput. Meth. Appl. Mech. Eng.*, **199**(21-22), 1371-1385. https://doi.org/10.1016/j.cma.2009.09.003.

Ethier, S.N and Kurtz, T.G. (2009), *Markov Processes: Characterization and Convergence*, Vol. 282, John Wiley & Sons.

Gasparini, A.M., Saetta, A.V. and Vitaliani, R.V. (1995), “On the stability and instability regions of non-conservative continuous system under partially follower forces”, *Comput. Meth. Appl. Mech. Eng.*, **124**, 63-78. https://doi.org/10.1016/0045-7825(94)00756-D.

Guckenheimer, J. and Holmes, Ph.J. (2013), *Nonlinear Oscillations, Dynamical Systems, and Bifurcations of Vector Fields*, Vol. 42, Springer.

Hajdo, E., Ibrahimbegovic, A. and Dolarevic, S. (2020), “Buckling analysis of complex structures with refined model built of frame and shell finite elements”, *Couple. Syst. Mech.*, **9**, 29-46. http://doi.org/10.12989/csm.2020.9.1.029.

Hajdo, E., Mejia-Nava, R.A., Imamovic, I. and Ibrahimbegovic, A. (2021), “Linearized instability analysis of frame structures under non-conservative loads: Static and dynamic approach”, *Couple. Syst. Mech.*, **10**, 79-102. https://doi.org/10.12989/csm.2021.10.1.079.

Ibrahimbegovic, A. (1995), “On FE implementation of geometrically nonlinear Reissner’s beam theory: Three-dimensional curved beam elements”, *Comput. Meth. Appl. Mech. Eng.*, **122**, 11-26.

Ibrahimbegovic, A. (1997), “On the choice of finite rotation parameters”, *Comput. Meth. Appl. Mech. Eng.*, **149**, 49-71. https://doi.org/10.1016/S0045-7825(97)00059-5.

Ibrahimbegovic, A. (2009), *Nonlinear Solid Mechanics: Theoretical Formulations and Finite Element Solution Methods*, Springer, Berlin, Germany.

Ibrahimbegovic, A. and Al Mikdad, M. (1998), “Finite rotations in dynamics of beams and implicit time-stepping schemes”, *Int. J. Numer. Meth. Eng.*, **41**, 781-814. https://doi.org/10.1002/(SICI)1097-0207(19980315)41:5<781::AID-NME308>3.0.CO;2-9.

Ibrahimbegovic, A. and Mamouri, S. (1999), “Nonlinear dynamics of flexible beams in planar motion: Formulation and time-stepping scheme for stiff problems”, *J. Comput. Struct.*, **70**, 1-21. https://doi.org/10.1016/S0045-7949(98)00150-3.

Ibrahimbegovic, A. and Taylor, R.L. (2002), “On the role of frame-invariance of structural mechanics models at finite rotations”, *Comput. Meth. Appl. Mech. Eng.*, **191**, 5159-5176. https://doi.org/10.1016/S0045-7825(02)00442-5.

Ibrahimbegovic, A., Hajdo, E. and Dolarevic, S. (2013), “Linear instability or buckling problems for mechanical and coupled thermomechanical extreme conditions”, *Couple. Syst. Mech.*, **2**, 349-374. http://doi.org/10.12989/csm.2013.2.4.349.

Ibrahmbegovic, A. and Mejia-Nava, R.A. (2021), “Heterogeneities and material-scales providing physically based damping to replace Rayleigh damping for any structure size”, *Couple. Syst. Mech.*, **10**, 201-216, http://doi.org/10.12989/csm.2021.10.3.201.

Imamovic, I., Ibrahimbegovic, A. and Hajdo, E. (2019), “Geometrically exact initially curved Kirchhoff’s planar elasto-plastic beam”, *Couple. Syst. Mech.*, **8**, 537-553. https://doi.org/10.12989/csm.2019.8.6.537.

Khasminskii, R. (2011), *Stochastic Stability of Differential Equations*, Vol. 66, Springer.

Kree, P. and Soize, Ch. (2012), *Mathematics of Random Phenomena: Random Vibrations of Mechanical Structures*, Vol. 32, Springer Science & Business Media.

Liptser, R. and Shiryayev, A.N. (2012), *Theory of Martingales*, Vol. 49, Springer.

Lozano, R., Brogliato, B., Egeland, O. and Maschke, B. (2000), *Dissipative Systems Analysis and Control: Theory and Applications*, Springer.

Masjedi, P.K. and Ovesy, H.R. (2015), “Large deflection analysis of geometrically exact spatial beams under conservative and nonconservative loads using intrinsic equation”, *Acta Mechanica*, **226**, 1689-1706. https://doi.org/10.1007/s00707-014-1281-3.

Medic, S., Dolarevic, S. and Ibrahimbegovic, A. (2013), “Beam model refinement and reduction”, *Eng. Struct.*, **50**, 158-169. https://doi.org/10.1016/j.engstruct.2012.10.004.
Mejia-Nava, A.R., Ibrahimbegovic, A. and Lozano, R. (2020), “Instability phenomena and their control in statics and dynamics: Application to deep and shallow truss and frame structure”, *Couple. Syst. Mech.*, **9**, 47-62. http://doi.org/10.12989/csm.2020.9.1.047.
Mejia-Nava, A.R., Imamovic, I., Hajdo, E. and Ibrahimbegovic, A. (2022), “Nonlinear instability problem for geometrically exact beam under conservative and non-conservative loads”, *Eng. Struct.* (in Press)
Moreno-Navarro, P., Ibrahimbegovic, A. and Damjanovic, D. (2021), “Multi-scale model for coupled piezoelectric-inelastic behavior”, *Couple. Syst. Mech.*, **10**(6), 521-544. https://doi.org/10.12989/csm.2021.10.6.521.
Parlett, B.N. (1980), *The Symmetric Eigenvalue Problem*, Prentice-Hall.
Timoshenko, S. and Gere, J.M. (1961), *Theory of Elastic Stability*, McGraw Hill.